Stereostructural and Vibrational Analyses of *cis*-Polyacetylene Based on Density Functional Calculations of Oligoenes

So Hirata, Hajime Torii, and Mitsuo Tasumi*

Department of Chemistry, School of Science, The University of Tokyo, Bunkyo-ku, Tokyo 113

(Received May 31, 1996)

The total energies and optimized structures of all-*trans*-transoid (*Tt*), all-*cis*-transoid (*Ct*), all-*trans*-cisoid (*Tc*), and all-*cis*-cisoid (*Cc*) oligoenes with various chain lengths were calculated using the Becke3–Lee–Yang–Parr (B3LYP) hybrid functional with the 6-31G* basis set. The optimized structures of the *Tt* and *Ct* oligoenes were found to be planer, whereas the *Tc* and *Cc* oligoenes have helical structures in which the conformations about the C–C bonds deviate from planar *s-cis*. The total energies of the *Tt*, *Ct*, *Tc*, and *Cc* oligoenes with the same chain length increase in this order. The vibrational force fields of the *Ct* and *Tc* oligoenes were calculated at the B3LYP/6-31G* level. The structures and force fields of the *Ct* and *Tc* polyacetylene were estimated by analyzing the chain-length dependence of the structural parameters and force constants of the oligoenes. The normal frequencies and the inelastic neutron scattering spectra were calculated for *Ct* and *Tc* polyacetylene on the basis of the thus-obtained structures and force fields. A comparison between the calculated and observed results clearly indicates that as-polymerized *cis*-rich polyacetylene consists of planar *Ct* chains. The comparison also suggests that the observed Raman bands of *cis*-rich polyacetylene films arise from *Ct* segments with intermediate conjugation lengths.

The spectroscopic properties of *cis*-polyacetylene (*cis*-rich polyacetylene, abbreviated as *cis*-PA) (Ref. 1) are significantly different from those of *trans*-polyacetylene (*trans*-rich polyacetylene, abbreviated as *trans*-PA). For example, the wavenumbers of the intense bands in the resonance Raman spectra of *trans*-PA are greatly dependent on the excitation wavelength,[2—8] while those of *cis*-PA are almost independent of it.[2,3,5,8,9] The resonance Raman spectra of *cis*-PA exhibit a long series of overtones and combinations as well as broad luminescence bands.[5,8—11] In the resonance Raman spectra of *trans*-PA, on the contrary, only a few overtones and combinations appear, and no luminescence band is observed.[5,8,10] The electronic absorption spectra of *cis*-PA have vibrational progressions, which cannot be seen in the electronic spectra of *trans*-PA.[2,4,12,13] To elucidate the origin of these differences between *cis*-PA and *trans*-PA, reliable vibrational force fields of both isomers in the ground and excited electronic states are required. In our pervious study,[14] normal coordinate analyses were performed for the all-*trans* form of PA in the ground electronic state on the basis of the force fields derived from ab initio molecular orbital calculations. It is not only of interest, but also of importance, to perform normal coordinate analyses for the all-*cis* form of PA on a similar theoretical basis.

As regular structures for PA, there are four possible forms with respect to the stereostructure about the C=C and C–C bonds: all-*trans*-transoid (*Tt*), all-*cis*-transoid (*Ct*), all-*trans*-cisoid (*Tc*), and all-*cis*-cisoid (*Cc*).[15] It has been established that *trans*-PA films mainly consist of planar *Tt* chains, based on the results of electron-diffraction studies,[16,17] an X-ray diffraction study,[18] and an infrared absorption study.[19] An X-ray diffraction study[20] and electron-diffraction studies[21,22] have also indicated that *cis*-PA films consist of planar chains in either the *Ct* or *Tc* form. Shirakawa et al.[12] have suggested that the chains in *cis*-PA films take the *Ct* form on the basis of empirical assignments of the resonance Raman bands. Bates and Baker have synthesized single crystals of a *cis*-PA–polystyrene diblock copolymer.[23] The structure of the single crystal (hexagonal, $a=5.12$ Å, $c=4.84$ Å)[23] is different from those reported for *cis*-PA films[20—22] (for example:[22] orthorhombic, $a=7.68$ Å, $b=4.46$ Å, $c=4.38$ Å). As an interpretation of this result, Bates and Baker have suggested that the single crystal which they have obtained consists of helical polyacetylene chains in a distorted *Cc* form (2*3/1 helices).

The energies of the oligoenes with various stereostructures have been calculated by the molecular orbital (MO) method as a part of studies on the stereostructure of polyacetylene.[24,25] Elert and White[24] have performed semiempirical MO calculations on the *Ct* and *Cc* oligoenes with 10 and 12 carbon atoms at the MNDO (modified neglect of diatomic overlap) level. Their result has indicated that a helical *Cc* oligoene is more stable than a planar *Ct* oligoene. Rao et al.[25] have calculated the energies of oligoenes with 6, 8, and 10 carbon atoms in the *Tt*, *Ct*, *Tc*, and *Cc* forms by the ab initio MO method at the Hartree–Fock (HF) level with the 4-31G basis set. They found that the total energies of the *Tt*, *Cc*, *Tc*, and *Ct* oligoenes with the same chain length increase in this order. Both of these studies have suggested that the planar *Ct* oligoenes spontaneously isomerize to the helical *Cc* oligoenes in solution. However, Rao et al.[25] have also demonstrated that the calculated results concerning the sta-

bility of the oligoenes are sensitive to the basis sets employed in the calculations. It is likely that the relative energies are sensitive to the theoretical levels as well as the basis sets. In order to obtain more accurate information about the relative energies of the oligoenes, it is necessary to calculate their total energies at fully optimized structures with a larger basis set and at an appropriate theoretical level.

Energetics is not the sole determinant of the stereostructure of polymers; it is also affected by the kinetics of polymerization. Vibrational spectroscopy is useful for studying the stereostructure of polymer chains in an actual sample. This is because some bands in the vibrational spectra of polymers change their positions substantially with the torsional angles about the C=C and C–C bonds. For *cis*-PA films, the infrared absorption spectra,[19,26–28] Raman spectra,[2–6,8,9,12,29–31] and inelastic neutron scattering (INS) spectra[32–34] have been observed. To derive structural information from these vibrational spectra, a reliable vibrational force field is required. Vibrational analyses of *cis*-PA[19,27,35–39] have been fewer in number than those of *trans*-PA, and most of them have dealt only with *Ct* PA. Vibrational analyses concerning *Ct* PA and *Tc* PA have been performed by Teramae et al.[38] on the basis of ab initio crystal orbital (CO) calculations at the HF/STO-3G level. Their analyses, however, have not taken into account the effect of electron correlation, which is known to play an important role in determining the vibrational frequencies of linear polyenes.[40]

The purpose of the present study was two fold. One was to calculate the relative energies of the *Tt*, *Ct*, *Tc*, and *Cc* oligoenes by a method which properly takes into account the effect of electron correlation and with a sufficiently large basis set. The other was to obtain reliable vibrational force fields of *Ct* PA and *Tc* PA, in order to examine quantitatively the experimental results for *cis*-PA. The total energies and optimized molecular structures for the *Tt*, *Ct*, *Tc*, and *Cc* oligoenes with various chain lengths were calculated using the Becke3–Lee–Yang–Parr (B3LYP) hybrid functional with the 6-31G* basis set. In the geometry optimizations of oligoenes, all of the structural degrees of freedom, including the torsional angles about the C=C and C–C bonds, were taken into account. The vibrational force fields were calculated for the *Ct* and *Tc* oligoenes with various chain lengths at the B3LYP/6-31G* level. The structural parameters and force constants of the *Ct* and *Tc* oligoenes were found to exhibit a systematic dependence on the chain length as well as the position in the chain. The chain-length dependence and position dependence of the structural parameters and force constants were analyzed quantitatively. The structural parameters and force constants of the infinite chains (*Ct* PA and *Tc* PA) were estimated on the basis of this analysis. Normal coordinate calculations were performed for *Ct* PA and *Tc* PA and their deuterated analogs with the thus-obtained structures and force fields. The wavenumbers for the infrared- and Raman-active modes and INS spectra were calculated for *Ct* PA and *Tc* PA, and compared with the experimental results. The origin of the difference between the excitation-wavelength dependence of the resonance Raman spectra of *cis*-PA and that of *trans*-PA is also discussed.

Method of Calculations

Density Functional Calculations and Normal Coordinate Analyses of Oligoenes. Density functional calculations of the *Tt*, *Ct*, *Tc*, and *Cc* oligoenes were performed using the Becke3–Lee–Yang–Parr (B3LYP) hybrid functional with the 6-31G* basis set with the Gaussian 94 program[41] on IBM SP2 workstations at the Computer Center of the Institute for Molecular Science. The total energies, optimized molecular structures, and vibrational force fields were calculated for butadiene, hexatriene, octatetraene, and decapentaene in the *Tt*, *Ct*, *Tc*, and *Cc* forms and for dodecahexaene and tetradecaheptaene in the *Tt*, *Ct*, and *Tc* forms. (All of the oligoenes treated in the present study have alternating C=C and C–C bonds, and the numbers indicating the position of the C=C bonds are omitted.) The optimized structures of the *Tt* and *Ct* oligoenes were found to be planar, while those of the *Tc* and *Cc* oligoenes were helical with the C–C bonds twisted from the planar *s-cis* form. No imaginary frequency was calculated for all of the species at the optimized structures. In the geometry optimization of dodecahexaene starting from the *Cc* form, the torsional angle about the central C–C bond changed from about 60° (*gauche*) to about 180° (*s-trans*), indicating the nonexistence of a potential energy minimum at the *Cc* form for dodecahexaene.

The force constants of the *Ct* and *Tc* oligoenes were transformed from the Cartesian-coordinate system to the group-coordinate system. The force constants in the group-coordinate system were then scaled. Vibrational frequency data of the *Ct* oligoenes have been observed for only hexatriene[42] and octatetraene.[43] For the normal (undeuterated) species of *Ct* octatetraene, the wavenumbers for only two skeletal stretching vibrations are available (1604 and 1260 cm^{-1}).[43] For the normal species of *Tc* hexatriene, only three infrared bands at 991, 974, and 908 cm^{-1} have been observed.[44] Therefore, the scale factors that could be determined uniquely by the observed data of the *Ct* and *Tc* oligoenes were limited in number. Hence, all of the force constants of the *Ct* and *Tc* oligoenes were uniformly scaled with a single scale factor of 0.9128. This value was determined by a least-squares fitting procedure so that wavenumbers calculated for the normal species of *Ct* hexatriene were in reasonable agreement with the observed values. The wavenumbers calculated at the B3LYP/6-31G* level for *Ct* hexatriene are shown in Table 1. The calculated wavenumbers are in agreement with the observed values with a mean absolute deviation of about 13 cm^{-1}. The calculated wavenumbers for the skeletal stretching vibrations of *Ct* octatetraene are 1617 and 1253 cm^{-1}. They are in reasonable agreement with the observed (1604 and 1260 cm^{-1}).[43] According to the calculations, three intense bands should be observed at 987, 969, and 886 cm^{-1} in the infrared spectra of *Tc* hexatriene. This result is also consistent with the previous observation.[44] The scale factor of 0.9128 was used to scale the force constants of all the oligoenes and polyacetylene treated in the present study.

Chain-Length Dependence and Position Dependence of the Structural Parameters and Force Constants of the All-*cis*-transoid and All-*trans*-cisoid Oligoenes. The chain-length dependence and position dependence of all the structural parameters and force constants calculated at the B3LYP/6-31G* level were analyzed quantitatively for the *Ct* and *Tc* oligoenes. On the basis of this analysis, the structures and force fields of *Ct* PA and *Tc* PA were derived.

Some structural parameters and force constants of the oligoenes converge rapidly as the chain length increases and the position becomes inner, thus the values associated with the central part of

Table 1. Wavenumbers for the Vibrational Modes of All-*cis*-transoid Hexatriene

Mode		Obsd[a]/cm^{-1}	Calcd/cm^{-1}	
			Unscaled	Scaled[b]
a_1	ν_1	3090	3247	3102
	ν_2		3180	3038
	ν_3	3011	3169	3028
	ν_4	2995	3161	3020
	ν_5	1626	1710	1634
	ν_6	1580	1644	1571
	ν_7	1397	1455	1390
	ν_8	1318	1358	1297
	ν_9	1247	1301	1243
	ν_{10}	1084	1112	1062
	ν_{11}	883	901	861
	ν_{12}	392	394	376
	ν_{13}	166	165	158
a_2	ν_{14}	(990)	1046	999
	ν_{15}	953	982	938
	ν_{16}	905	924	883
	ν_{17}	705	733	700
	ν_{18}	331	333	318
	ν_{19}	155	157	150
b_1	ν_{20}	3089	3247	3102
	ν_{21}	3045	3167	3026
	ν_{22}	3014	3161	3020
	ν_{23}	2979	3147	3007
	ν_{24}	1616	1702	1626
	ν_{25}	1449	1509	1442
	ν_{26}	1355	1406	1343
	ν_{27}	1279	1320	1261
	ν_{28}	1185	1225	1170
	ν_{29}	950	973	930
	ν_{30}	(675)	689	658
	ν_{31}	356	351	335
b_2	ν_{32}	989	1032	986
	ν_{33}	906	926	885
	ν_{34}	815	851	813
	ν_{35}	590	608	581
	ν_{36}	100	106	101

a) Ref. 42. b) The force constants are calculated at the B3LYP/6-31G* level and then uniformly scaled by 0.9128.

tetradecaheptaene can be transferred directly to the infinite chains (*Ct* PA and *Tc* PA). For the other structural parameters and force constants, the values associated with the central part of tetradecaheptaene cannot be regarded as being equal to those of the infinite chains, since their convergence is relatively slow. The C–C torsional angles of the *Tc* oligoenes, the skeletal bond lengths of the *Ct* and *Tc* oligoenes, and the skeletal stretching force constants of the *Ct* and *Tc* oligoenes are included in the latter category. The structural parameters and force constants of the infinite chains in this category were extrapolated from those of the oligoenes by the following procedure. The structural parameters and force constants of the oligoenes were approximated by functions having parameters n and i, representing, respectively, the chain length and the position in the chain. For the off-diagonal force constants, another parameter (j), representing the distance between the two groups associated with the constant, was also used in the functions. Parameter n was defined as the number of C=C bonds in the oligoenes. The structural parameters and force constants at both ends of the oligoenes were numbered as $i=1$ and the other structural parameters and force constants were numbered as $i=2,3,\cdots$, as the position goes toward the center. The numbering is illustrated in Fig. 1 for the C=C and C–C bonds in the *Ct* oligoenes. The off-diagonal force constants were numbered as $j=1$ when two neighboring groups are associated with the constant, and as $j=2,3,\cdots$, as the two groups become distant (Fig. 1). The skeletal bond lengths and the associated force constants of the *Ct* and *Tc* oligoenes were well approximated by functions having the same form as those used to express the corresponding structural parameters and force constants of the *Tt* oligoenes.[14] The values of the parameters in the functions were determined by a least-squares fitting procedure with the Statistical Analysis with Least Squares Fitting (SALS) subroutine[45] to obtain good fits between the values calculated with the functions and those obtained from the density functional calculations. The values of the parameters for the *Ct* and *Tc* oligoenes are summarized in the Appendix. The structural parameters and force constants of the infinite chains were obtained by substituting infinity for n and i in the functions.

It is probable that the wavenumbers for the skeletal stretching vibrations (and the associated force constants) of the *Ct* and *Tc* oligoenes converge more rapidly than those of the *Tt* oligoenes.[46] Thus, it may not be valid to approximate the skeletal stretching force constants of the *Ct* and *Tc* oligoenes by the same functions (with different values of parameters) as those used to approximate the corresponding force constants of the *Tt* oligoenes. Hence, we derived another force field for *Ct* PA and *Tc* PA by directly transferring the force constants associated with the central part of tetradecaheptaene.

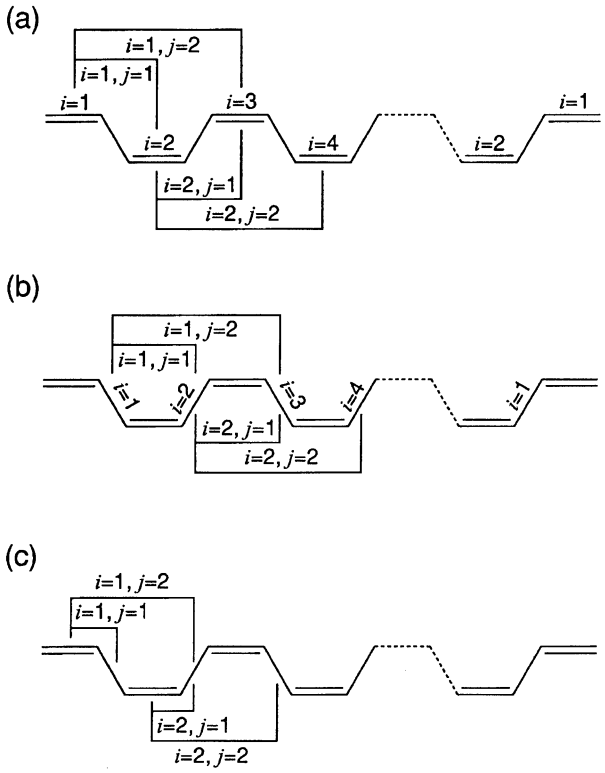

Fig. 1. (a) Numbering of the C=C bonds and the C=C stretch/C=C stretch interaction constants in all-*cis*-transoid oligoenes. (b) Numbering of the C–C bonds and the C–C stretch/C–C stretch interaction constants in all-*cis*-transoid oligoenes. (c) Numbering of the C=C stretch/C–C stretch interaction constants in all-*cis*-transoid oligoenes.

Hereafter, we refer to the force field obtained by extrapolation as force field I, and the other force field as force field II. Force field I differs from force field II only in the skeletal stretching force constants, since all of the other force constants in both of these force fields were directly transferred from those of tetradecaheptaene. (All of the force constants, other than the skeletal stretching force constants, rapidly converge as the chain length increases, and, hence, the values associated with the central part of tetradecaheptaene can be safely regarded as being equal to those of the infinite chain.)

All of the force constants thus-obtained for *Ct* PA and *Tc* PA were scaled by a single scale factor of 0.9128. The force constants mentioned hereafter, including those of the oligoenes, are scaled.

Normal Coordinate Analyses of All-*cis*-transoid and All-*trans*-cisoid Polyacetylene. Normal coordinate analyses were performed for *Ct* PA, *Tc* PA, and their deuterated analogs on a HITAC M880/310 computer at the Computer Centre of the University of Tokyo. On the basis of the analysis of the optimized molecular structures of the oligoenes, the planarity of *Ct* PA and *Tc* PA was assumed (vide post).

The group coordinates given in Table 2 were defined according to the IUPAC recommendations.[47] In normal coordinate analyses of polymers it is convenient to define a coordinate system in which a right-handed Cartesian-coordinate system is fixed to each repeating unit (C_2H_2); the z-axis coincides with the chain direction, and the x- and y-axes are in and out of the molecular plane, respectively, as shown in Fig. 2. The force constants of *Ct* PA and *Tc* PA were transformed from the group-coordinate system to this Cartesian-coordinate system. The 12×12 dynamical matrices corresponding to the vibrational phase differences (δ) between adjacent repeating units were constructed on the Cartesian-coordinate basis. The eigenvalues and eigenvectors of the dynamical matrices were calculated by changing the δ value.

For the infinite chains of planar *Ct* PA and *Tc* PA, the vibrational modes at $\delta = 0$ or $\delta = \pi$ are infrared- or Raman-active.[48] The wavenumbers for the $\delta = 0$ and $\delta = \pi$ modes were calculated for *Ct* $(CH)_x$, *Tc* $(CH)_x$, *Ct* $(CD)_x$, and *Tc* $(CD)_x$. Force fields I and II were used in combination with the structural parameters obtained by extrapolation. The values of the potential energy distributions (PEDs) were calculated for the $\delta = 0$ and $\delta = \pi$ vibrations of *Ct* $(CH)_x$ and *Ct* $(CD)_x$. The vibrational patterns of the $\delta = 0$ and $\delta = \pi$ modes were drawn for *Ct* $(CH)_x$ with the LXVIEW program.[49] The phonon dispersion curves of *Ct* $(CH)_x$ and *Ct* $(CD)_x$, the density of vibrational states of *Ct* $(CH)_x$ and *Ct* $(CD)_x$, and the hydrogen-amplitude-weighted density of states of *Ct* $(CH)_x$ and *Tc* $(CH)_x$ were calculated in the same manner as in Ref. 14.

Results and Discussion

Total Energies and Optimized Molecular Structures of the All-*cis*-transoid, All-*trans*-cisoid, and All-*cis*-cisoid Oligoenes. The optimized molecular structures of the *Ct* oligoenes are planar. In contrast, the *Tc* and *Cc* oligoenes have helical structures in which the conformations about the C–C bonds substantially deviate from planar *s-cis*, probably due to a hydrogen–hydrogen nonbonded repulsion. The CC=CC groups of the *Tc* oligoenes remain almost planar with

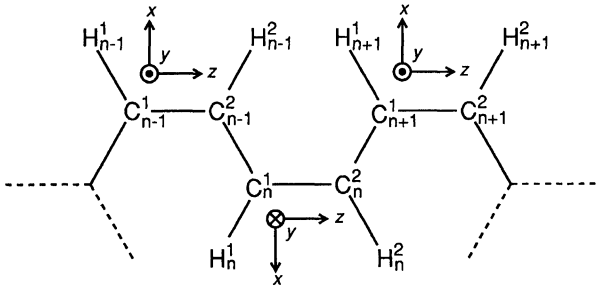

Fig. 2. Numbering of atoms in all-*cis*-transoid and all-*trans*-cisoid polyacetylene. Subscript n indicates that the atoms belong to the nth repeating unit. Right-handed Cartesian-coordinate systems fixed to repeating units are also shown.

Table 2. Group Coordinates of All-*cis*-transoid and All-*trans*-cisoid Polyacetylene

Group coordinate[a,b,c]	
$S^1_n = \Delta r\left(C^1_n - C^2_n\right)$	CC stretch
$S^2_n = \Delta r\left(C^2_{n-1} - C^1_n\right)$	CC stretch
$S^3_n = \Delta r\left(C^1_n - H^1_n\right)$	CH stretch
$S^4_n = \Delta r\left(C^2_n - H^2_n\right)$	CH stretch
$S^5_n = 2^{-1/2}\left(\Delta\angle C^2_nC^1_nH^1_n - \Delta\angle C^2_{n-1}C^1_nH^1_n\right)$	CH in-plane bend
$S^6_n = 2^{-1/2}\left(\Delta\angle C^1_nC^2_nH^2_n - \Delta\angle C^1_{n+1}C^2_nH^2_n\right)$	CH in-plane bend
$S^7_n = 6^{-1/2}\left(2\Delta\angle C^2_{n-1}C^1_nC^2_n - \Delta\angle C^2_nC^1_nH^1_n - \Delta\angle C^2_{n-1}C^1_nH^1_n\right)$	CCC deformation
$S^8_n = 6^{-1/2}\left(2\Delta\angle C^1_{n+1}C^2_nC^1_n - \Delta\angle C^1_nC^2_nH^2_n - \Delta\angle C^1_{n+1}C^2_nH^2_n\right)$	CCC deformation
$S^9_n = \Delta\pi\left(C^1_n\text{–}H^1_n\right)\sin\angle C^2_{n-1}C^1_nC^2_n$	CH out-of-plane wag
$S^{10}_n = \Delta\pi\left(C^2_n\text{–}H^2_n\right)\sin\angle C^1_{n+1}C^2_nC^1_n$	CH out-of-plane wag
$S^{11}_n = 4^{-1}\left\{\Delta\tau\left(H^1_nC^1_n\text{–}C^2_nH^2_n\right) + \Delta\tau\left(C^2_{n-1}C^1_n\text{–}C^2_nH^2_n\right) + \Delta\tau\left(H^1_nC^1_n\text{–}C^2_nC^1_{n+1}\right) + \Delta\tau\left(C^2_{n-1}C^1_n\text{–}C^2_nC^1_{n+1}\right)\right\}$	CC torsion
$S^{12}_n = 4^{-1}\left\{\Delta\tau\left(H^2_{n-1}C^2_{n-1}\text{–}C^1_nH^1_n\right) + \Delta\tau\left(C^1_{n-1}C^2_{n-1}\text{–}C^1_nH^1_n\right) + \Delta\tau\left(H^2_{n-1}C^2_{n-1}\text{–}C^1_nC^2_n\right) + \Delta\tau\left(C^1_{n-1}C^2_{n-1}\text{–}C^1_nC^2_n\right)\right\}$	CC torsion

a) As for the numbering of the carbon and hydrogen atoms, see Fig. 2. b) Subscript n refers to the numbering of the repeating units. c) The coordinates Δr(X–Y), $\Delta\angle$XCY, $\Delta\pi$(C–H), and $\Delta\tau$(XC–CY) denotes, respectively, the change in the X–Y bond length, the change in the angle between the XC and CY bonds, the change in the angle between the C–H bond and the plane defined by the carbon skeleton, and the change in the individual dihedral angle between the XC and CY bonds. The sign of the coordinate $\Delta\pi$(C–H) is taken to be positive if the hydrogen atoms move in the $+y$ direction in Fig. 2. As for the sign of the coordinate $\Delta\tau$(XC–CY), see Ref. 47.

a deviation from planarity being 3.2° at maximum. For the *Cc* oligoenes, the maximum deviation is as much as 6.2°, implying a larger steric repulsion. The C–C torsional angles of the *Tc* and *Cc* oligoenes are summarized in Table 3.

The total energies and energies relative to the *Tt* oligoenes are listed in Table 4 for the *Tt*, *Ct*, *Tc*, and *Cc* oligoenes. The *Cc* oligoenes are found to be most unstable, and the total energies decrease in the order $Cc > Tc > Ct > Tt$. The relative energies of the *Cc* oligoenes increase rapidly from 16.6 kJ mol^{-1} to 23.2 kJ mol^{-1} on going from hexatriene to decapentaene. As a consequence, dodecahexaene does not exist in the *Cc* form; the internal-rotation potential about the central C–C bond of *Cc* dodecahexaene has no local minimum at the *gauche* form. We confirmed this point by calculating the potential energy curve about the central C–C bond for *Cc* dodecahexaene at each of eight fixed CC–CC dihedral angles (40°, 50°, 60°, 70°, 90°, 120°, 150°, and 180°) by optimizing all other structural parameters. The calculated potential energy curve has a shoulder (not a minimum) at about 60°, and a deep minimum at 180°, corresponding to the *s-trans* form of the central C–C bond. This means that the *Ct* form is much more stable than the *Cc* form. The present result casts doubt on the existence of a helical *Cc* PA, which was proposed in previous studies.[23–25]

The energies per C_2H_2 unit of *Ct* and *Tc* tetradecaheptaene are higher than that of *Tt* tetradecaheptaene by 6.4 and 12.9 kJ mol^{-1}, respectively. These values are comparable with those of *Ct* PA and *Tc* PA relative to *Tt* PA (8.7 and 15.0 kJ mol^{-1}, respectively) calculated by Teramae[50] using the ab initio CO method at the HF/4-31G level.

Chain-Length Dependence and Position Dependence of the Structural Parameters. In the *Tc* oligoenes, the conformations about the C–C bonds significantly deviate from planar *s-cis*. As shown in Table 3, the C–C torsional angles strongly depend on the chain length. The structures about the C=C bonds, on the other hand, remain almost planar, and the C=C torsional angles do not exhibit a significant chain-length dependence. Since the *Ct* oligoenes are planar molecules, their C=C and C–C torsional angles are also independent of the chain length.

The C–C torsional angles of the *Tc* oligoenes (hereafter abbreviated as τ_{C-C}'s), calculated at the B3LYP/6-31G* level, are plotted against n in Fig. 3. The τ_{C-C}'s decrease systematically with increasing n and i. This decrease is probably a consequence of an increase in the degree of π-electron conjugation with increasing n and i. The τ_{C-C}'s associated with the central parts of the *Tc* oligoenes are expected to approach that of an infinite *Tc* PA chain as $n \rightarrow \infty$. However, since the convergence is relatively slow, the central τ_{C-C} of *Tc* tetradecaheptaene cannot be regarded as being equal to the τ_{C-C} of *Tc* PA. In order to obtain the τ_{C-C} of *Tc* PA, we approximated the τ_{C-C}'s of the *Tc* oligoenes by a function of n and i. The functional form and the values of the parameters in the function are given in the Appendix. The τ_{C-C}'s calculated with the function are in satisfactory agreement with those calculated at the B3LYP/6-31G* level (Fig. 3). The τ_{C-C} of *Tc* PA was found to be 2.82° by substituting infinity for n and i in the function. Thus, it is likely that *Tc* PA has either a planar structure or a form close to it. If the deviation from planarity is small, no significant differences would take

Table 3. C–C Torsional Angles of All-*trans*-cisoid and All-*cis*-cisoid Oligoenes[a,b]

Molecule	All-*trans*-cisoid			All-*cis*-cisoid		
	$i=1$	$i=2$	$i=3$	$i=1$	$i=2$	$i=3$
Butadiene	30.2			30.2		
Hexatriene	25.8			35.6		
Octatetraene	23.7	22.0		7.3	42.8	
Decapentaene	23.1	20.1		31.0	59.0	
Dodecahexaene	22.1	18.7	17.7			
Tetradecaheptaene	21.7	18.2	16.5			

a) In units of degrees. b) As for the numbering of the C–C bonds, see Fig. 1b.

Table 4. Total and Relative Energies of All-*trans*-transoid, All-*cis*-transoid, All-*trans*-cisoid, and All-*cis*-cisoid Oligoenes[a]

Molecule	All-*trans*-transoid		All-*cis*-transoid		All-*trans*-cisoid		All-*cis*-cisoid	
	E	ΔE	E	ΔE	E	ΔE	E	ΔE
Butadiene	−155.99214	0.0	b)	b)	−155.98648	7.4	c)	c)
Hexatriene	−233.39855	0.0	−233.39551	2.7	−233.38720	9.9	−233.37956	16.6
Octatetraene	−310.80566	0.0	−310.79924	4.2	−310.78854	11.2	−310.77688	18.9
Decapentaene	−388.21308	0.0	−388.20313	5.2	−388.19016	12.0	−388.16895	23.2
Dodecahexaene	−465.62065	0.0	−465.60712	5.9	−465.59194	12.6		
Tetradecaheptaene	−543.02832	0.0	−543.01114	6.4	−542.99383	12.9		

a) Total energies (E) in atomic unit, and energies relative to the *trans*-transoid conformation (ΔE) in kJ mol^{-1} per C_2H_2 unit. All the structural parameters are optimized. b) *Cis*-transoid butadiene is identical with *trans*-transoid butadiene. c) *Cis*-cisoid butadiene is identical with *trans*-cisoid butadiene.

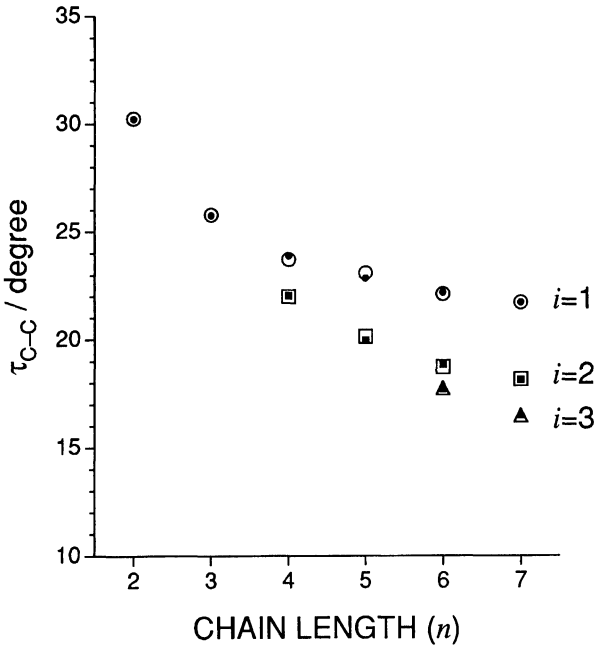

Fig. 3. The C–C torsional angles (τ_{C-C}'s) of all-*trans*-cisoid oligoenes as a function of chain length. The τ_{C-C}'s calculated at the B3LYP/6-31G* level are indicated by open marks, and those calculated with the function given in the Appendix by filled marks. As for the numbering of the C–C bonds, see Fig. 1b.

place between the vibrational frequencies calculated for a planar form and those calculated for a deviated form. In a later section, the vibrational frequencies of *Tc* PA in a planar form are discussed.

The C=C bond lengths ($r_{C=C}$'s) and the C–C bond lengths (r_{C-C}'s) calculated at the B3LYP/6-31G* level are plotted against n in Figs. 4 and 5, respectively, for the *Ct* and *Tc* oligoenes. As can be clearly seen in Fig. 4, the chain-length dependence and the position dependence of the $r_{C=C}$'s of the *Ct* oligoenes are qualitatively the same as those of the *Tc* oligoenes. They are also similar to those of the *Tt* oligoenes.[14] Hence, the $r_{C=C}$'s of the *Ct* and *Tc* oligoenes are well approximated by the same function (with different values of the parameters) as that used for the $r_{C=C}$'s of the *Tt* oligoenes. The r_{C-C}'s of the *Ct* oligoenes also exhibit qualitatively the same chain-length and position dependence as those of the *Tc* oligoenes, as shown in Fig. 5. However, the r_{C-C}'s of the *Tc* oligoenes are substantially longer than the corresponding r_{C-C}'s of the *Ct* oligoenes. This is because the C–C bonds of the *Tc* oligoenes, which are twisted from the planar *s-cis* form, have a less C=C bond-like character than those of the *Ct* oligoenes. The $r_{C=C}$'s of the *Tc* oligoenes are only slightly shorter than the corresponding $r_{C=C}$'s of the *Ct* oligoenes; the effect of the deviation from planarity is less appreciable on the $r_{C=C}$'s than on the r_{C-C}'s. The r_{C-C}'s of the *Ct* and *Tc* oligoenes are approximated by functions of n and i. The functions have the same form as that for the r_{C-C}'s in the *Tt* oligoenes (see Appendix).

The $r_{C=C}$ and r_{C-C} of *Ct* PA and *Tc* PA are extrapolated by substituting infinity for n and i in the functions which approximate the corresponding bond lengths of the oligoenes. Since the C–H bond lengths, CCC angles, and C=CH angles of the *Ct* and *Tc* oligoenes converge rapidly as the chain length increases, the bond lengths and angles in the central part of tetradecaheptaene are adopted as those of polyacetylene. The structures thus-obtained for *Ct* PA and *Tc* PA are shown in Table 5. The value of the $r_{C=C}$ of a *cis*-PA film, measured by nutation NMR spectroscopy, is 1.37 Å.[51] The $r_{C=C}$'s of *Ct* PA and *Tc* PA, obtained by extrapolation, are 1.374 and 1.377 Å, respectively; both of them are in agreement with the observed value (1.37 Å). The $r_{C=C}$ of polyacetylene is

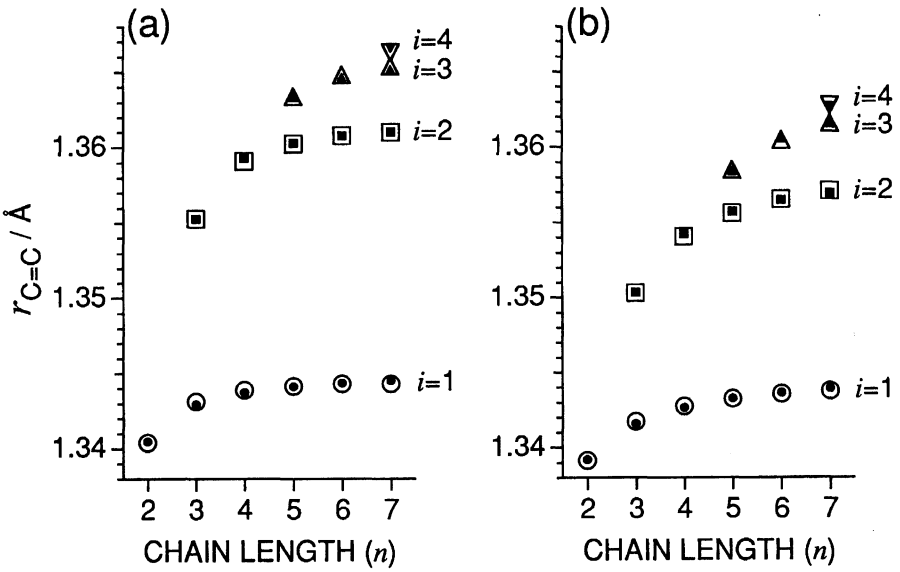

Fig. 4. The C=C bond lengths ($r_{C=C}$'s) of (a) all-*cis*-transoid and (b) all-*trans*-cisoid oligoenes as a function of chain length. The $r_{C=C}$'s calculated at the B3LYP/6-31G* level are indicated by open marks, and those calculated with the function given in the Appendix by filled marks. As for the numbering of the C=C bonds, see Fig. 1a.

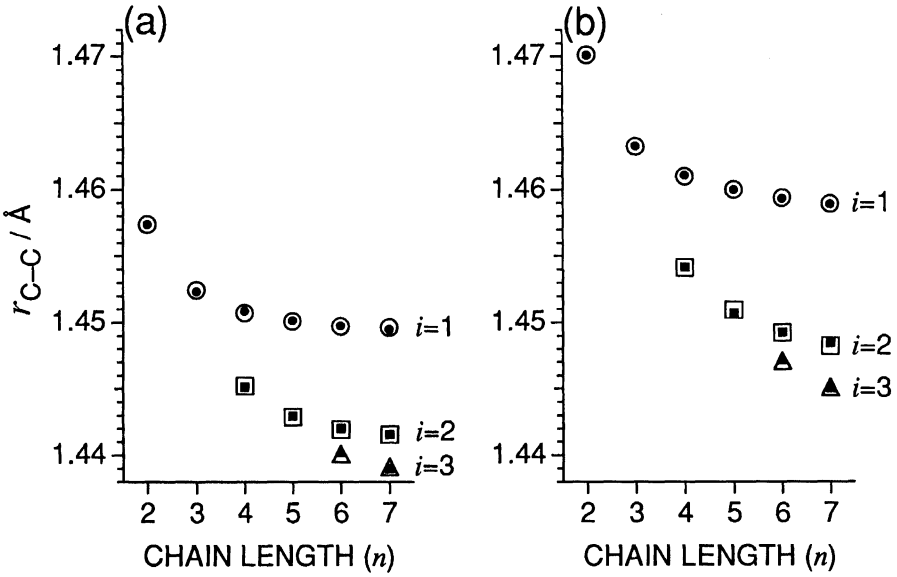

Fig. 5. The C–C bond lengths (r_{C-C}'s) of (a) all-*cis*-transoid and (b) all-*trans*-cisoid oligoenes as a function of chain length, plotted in a similar way as in Fig. 4. As for the numbering of the C–C bonds, see Fig. 1b.

Table 5. Calculated Structural Parameters of All-*cis*-transoid and All-*trans*-cisoid Polyacetylene[a)]

Structural parameter	All-*cis*-transoid	All-*trans*-cisoid
C=C bond length	1.374	1.377
C–C bond length	1.429	1.429
CH bond length	1.087	1.089
CCC angle	126.8	126.6
C=CH angle	116.4	118.0

a) In units of Å (bond length) and degrees (bond angles).

longer than the central $r_{C=C}$ of tetradecaheptaene by 0.008 Å for the *Ct* form and by 0.014 Å for the *Tc* form. Thus, the magnitude of the chain-length dependence and the position dependence of the $r_{C=C}$'s is larger in the *Tc* form than in the *Ct* form. Correspondingly, the difference between the r_{C-C} of *Tc* PA and the central r_{C-C} of *Tc* tetradecaheptaene (0.016 Å) is larger than that for the *Ct* form (0.010 Å). The larger chain-length and position dependence in the *Tc* form than in the *Ct* form can be explained as follows. The τ_{C-C}'s of the *Tc* oligoenes decrease as the degree of π-electron conjugation increases. The decrease in the τ_{C-C}'s further increases the degree of π-electron conjugation. Due to this mutual effect in *Tc* oligoenes, the degree of π-electron conjugation varies greatly with the chain length and position.

The optimized structures of *Ct* PA and *Tc* PA were obtained at the HF/4-31G level by Teramae.[50)] The $r_{C=C}$'s of *Ct* PA and *Tc* PA at the HF/4-31G level are 1.337 and 1.333 Å, respectively, and are considerably shorter than the corresponding values estimated at the B3LYP/6-31G* level. The r_{C-C}'s of *Ct* PA and *Tc* PA at the HF/4-31G level (1.452 and 1.460 Å, respectively) are, on the other hand, longer than those at the B3LYP/6-31G* level. These differences are likely to be due partly to the use of different basis set, and partly to the effect of electron correlation, in analogy with the case of *Tt* PA, in which the degree of bond alternation has been shown to decrease by the inclusion of electron correlation.[52)]

Chain-Length Dependence and Position Dependence of the Force Constants. The values of the C=C stretching force constants ($f_{C=C}$'s) of the *Ct* and *Tc* oligoenes are plotted against *n* in Fig. 6, and the values of the C–C stretching force constants (f_{C-C}'s) of the *Ct* and *Tc* oligoenes are plotted against *n* in Fig. 7. The $f_{C=C}$'s (f_{C-C}'s) associated with the central parts of the *Ct* and *Tc* oligoenes are the smallest (largest) among the $f_{C=C}$'s (f_{C-C}'s) in a chain. The central $f_{C=C}$'s and f_{C-C}'s are expected to approach those of the infinite chains as $n\rightarrow\infty$. However, since their convergence is slow, the central $f_{C=C}$ and f_{C-C} of tetradecaheptaene cannot be regarded as being equal to those of the infinite chains.

The magnitude of the chain-length dependence and the position dependence of $f_{C=C}$'s and f_{C-C}'s are larger in the *Tc* oligoenes than in the *Ct* oligoenes, parallel to the case of the $r_{C=C}$'s and r_{C-C}'s (see the previous subsection). Using the functions given in the Appendix, we have found that the $f_{C=C}$ and f_{C-C} of *Ct* PA (force field I) are 7.310 and 5.351 mdyn Å^{-1}, respectively. The $f_{C=C}$ and f_{C-C} of *Tc* PA (force field I) are likewise evaluated to be 6.908 and 5.474 mdyn Å^{-1}, respectively.

The values of the skeletal-stretch interaction constants, i.e., $f_{C=C/C=C}$'s, $f_{C-C/C-C}$'s, and $f_{C=C/C-C}$'s, are plotted against *n* in Figs. 8, 9, and 10, respectively, for the *Ct* and *Tc* oligoenes. In Fig. 10, only the $f_{C=C/C-C}$'s associated with the central part of the oligoenes are shown for the sake of simplicity. Since none of these three interaction constants associated with the central parts of the oligoenes converge rapidly, the values associated with the central part of tetradecaheptaene cannot be regarded as being equal to those of the infinite chains. These interaction constants of the *Ct* and *Tc* oligoenes are again satisfactorily approximated by the same functions (with different values of the parameters) as those used for the corresponding interaction constants of the *Tt* oligoenes (see Appendix). By substituting infinity for *n* and *i* in the

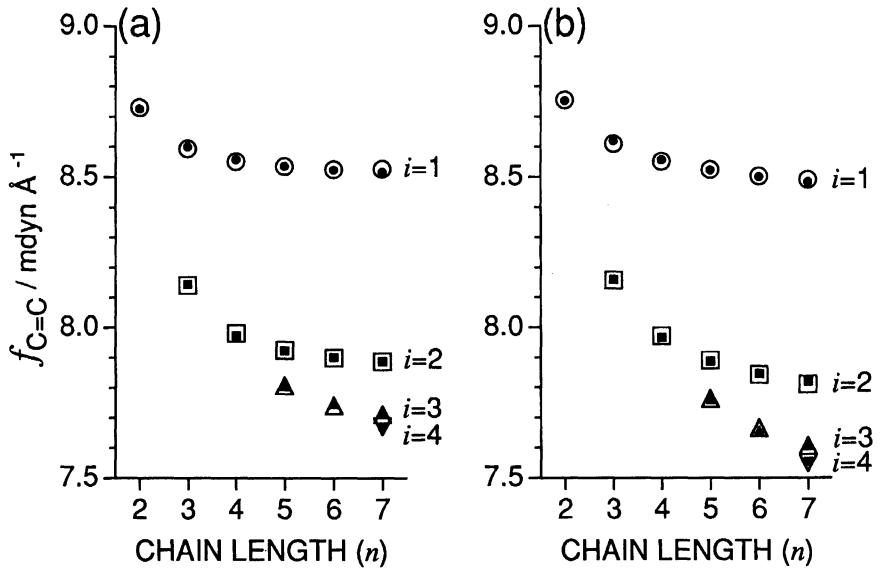

Fig. 6. The scaled C=C stretching force constants ($f_{C=C}$'s) of (a) all-*cis*-transoid and (b) all-*trans*-cisoid oligoenes as a function of chain length, plotted in a similar way as in Fig. 4. As for the numbering of the C=C bonds, see Fig. 1a.

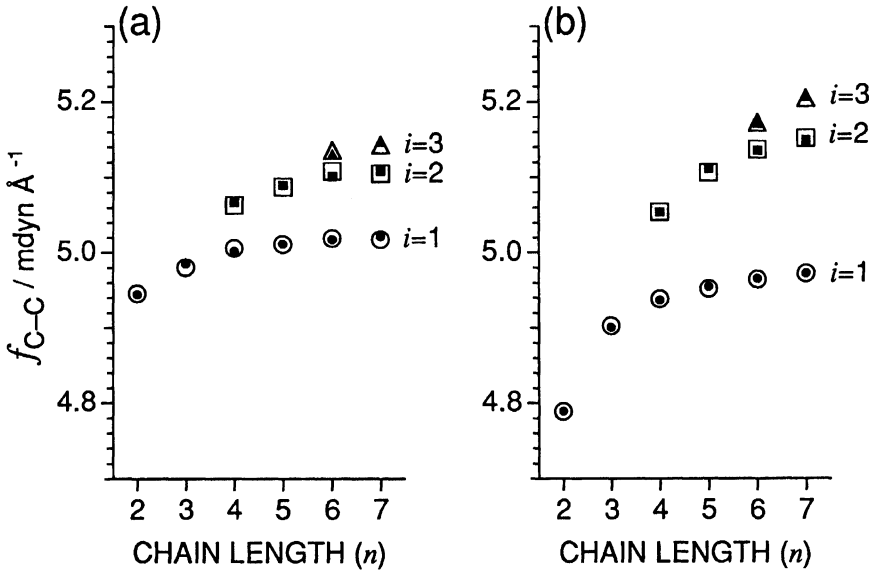

Fig. 7. The scaled C–C stretching force constants (f_{C-C}'s) of (a) all-*cis*-transoid and (b) all-*trans*-cisoid oligoenes as a function of chain length, plotted in a similar way as in Fig. 4. As for the numbering of the C–C bonds, see Fig. 1b.

functions, the interaction constants of force field I can be obtained.

Vibrational Analyses of All-*cis*-transoid and All-*trans*-cisoid Polyacetylene. Two force fields (I and II) were obtained for each of *Ct* PA and *Tc* PA on the basis of the analysis described in the previous subsection. The values of the force constants are listed in Table 6 for force field II of *Ct* PA. Force field I of *Ct* PA is obtained by replacing the diagonal and off-diagonal skeletal stretching force constants listed in Table 6 by those obtained by substituting infinity for n and i in the functions given in the Appendix.

The wavenumbers calculated for the $\delta = 0$ and $\delta = \pi$ modes of *Ct* $(CH)_x$ and *Ct* $(CD)_x$ with force fields I and II are shown in Table 7. The calculated wavenumbers are compared with the wavenumbers of the observed infrared and Raman bands of *cis*-PA films.[6,9,19,26] The values of the potential energy distributions (PEDs) in Table 7 were calculated with force field II. The vibrational patterns of the $\delta = 0$ and $\delta = \pi$ modes of *Ct* $(CH)_x$ calculated with force field II are shown in Fig. 11. The wavenumbers calculated for the $\delta = 0$ and $\delta = \pi$ modes of *Tc* $(CH)_x$ and *Tc* $(CD)_x$ with force fields I and II are given in Table 8.

Comparing the wavenumbers calculated for the modes of *Ct* PA with those of *Tc* PA, we have found that the wavenumbers for some modes are significantly affected by the stereostructures about the C=C and C–C bonds. These modes will be useful in discussing the correlation between the vibrational spectra and the stereostructure of the polymer, if they give rise to sufficiently intense bands. For *cis*-PA, such vibrational modes are the skeletal stretching vibrations (ν_2

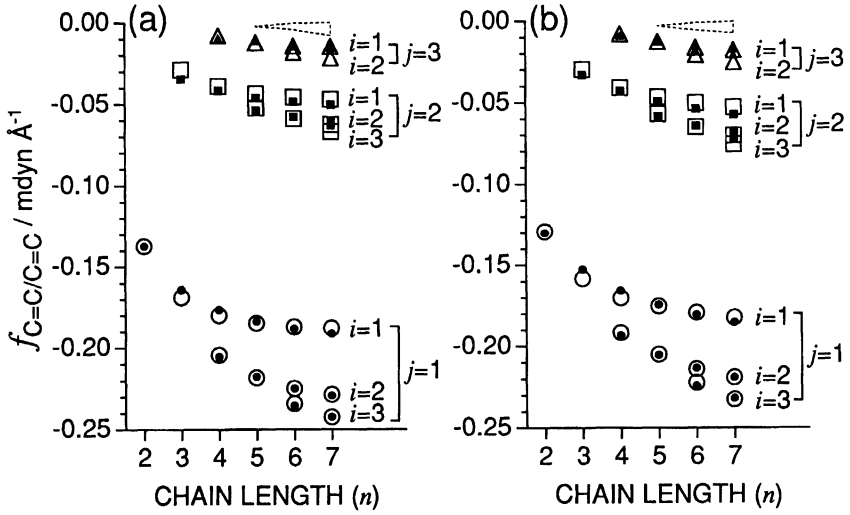

Fig. 8. The scaled C=C stretch/C=C stretch interaction constants ($f_{C=C/C=C}$'s) of (a) all-*cis*-transoid and (b) all-*trans*-cisoid oligoenes as a function of chain length. The $f_{C=C/C=C}$'s calculated at the B3LYP/6-31G* level are indicated by open marks, and the $f_{C=C/C=C}$'s calculated with the function given in the Appendix by filled marks. Only the $f_{C=C/C=C}$'s with $j = 1$, 2, and 3 are shown for the sake of simplicity. The $f_{C=C/C=C}$'s with j greater than 3 have their values in the region surrounded by the broken lines. As for the numbering of the $f_{C=C/C=C}$'s, see Fig. 1a.

Table 6. Scaled Force Constants (Force Field II) of All-*cis*-transoid Polyacetylene in the Group-Coordinate System[a,b,c,d,e]

(In-plane force constants)

	S_n^1	S_n^2	S_n^3	S_n^4	S_n^5	S_n^6	S_n^7	S_n^8
S_n^1	7.670	0.600	0.087	0.087	0.207	0.207	0.241	0.241
S_n^2	0.600	5.143	0.072	−0.009	−0.171	0.033	0.171	0.028
S_n^3	0.087	0.072	5.074	0.014	0.019	−0.013	−0.091	0.038
S_n^4	0.087	−0.009	0.014	5.074	−0.013	0.019	0.038	−0.091
S_n^5	0.207	−0.171	0.019	−0.013	0.542	0.001	−0.007	0.040
S_n^6	0.207	0.033	−0.013	0.019	0.001	0.542	0.040	−0.007
S_n^7	0.241	0.171	−0.091	0.038	−0.007	0.040	0.824	0.158
S_n^8	0.241	0.028	0.038	−0.091	0.040	−0.007	0.158	0.824

	S_{n+1}^1	S_{n+1}^2	S_{n+1}^3	S_{n+1}^4	S_{n+1}^5	S_{n+1}^6	S_{n+1}^7	S_{n+1}^8
S_n^1	−0.242	0.600	−0.045	0.006	−0.034	0.004	−0.004	−0.011
S_n^2	0.094	−0.128	0.004	0.001	−0.026	0.002	−0.007	
S_n^3	0.006	−0.009		0.002	0.003	0.003	0.008	−0.003
S_n^4	−0.045	0.072	−0.002		−0.024	0.002	−0.108	−0.061
S_n^5	0.004	0.033	0.002	0.003	−0.001	0.003	0.013	−0.002
S_n^6	−0.034	−0.171	−0.024	0.003	0.039	−0.008	−0.009	−0.052
S_n^7	−0.012	0.028	−0.061	−0.003	−0.052	−0.002	−0.029	0.018
S_n^8	−0.004	0.171	−0.108	0.008	−0.009	0.013	0.040	−0.029

	S_{n+2}^1	S_{n+2}^2	S_{n+2}^3	S_{n+2}^4	S_{n+2}^5	S_{n+2}^6	S_{n+2}^7	S_{n+2}^8
S_n^1	−0.067	0.094	−0.002		0.002		−0.003	
S_n^2	0.029	−0.039	−0.001		0.002			
S_n^3		0.001					0.002	
S_n^4	−0.002	0.004	0.030		0.003		0.011	−0.003
S_n^5		0.002						
S_n^6	0.002	−0.026	0.003		0.024		0.008	0.002
S_n^7			−0.003		0.002			
S_n^8	−0.003	−0.007	0.011	0.002	0.008		0.005	

	S_{n+3}^1	S_{n+3}^2	S_{n+3}^3	S_{n+3}^4	S_{n+3}^5	S_{n+3}^6	S_{n+3}^7	S_{n+3}^8
S_n^1	−0.022	0.029						
S_n^2	0.009	−0.013						
S_n^3								
S_n^4		−0.001						
S_n^5								
S_n^6		0.002						
S_n^7								
S_n^8								

	S_{n+4}^1	S_{n+4}^2	S_{n+5}^1	S_{n+5}^2
S_n^1	−0.008	0.009	−0.002	0.003
S_n^2	0.003	−0.003		−0.001

(Out-of-plane force constants)

	S_n^9	S_n^{10}	S_n^{11}	S_n^{12}	S_{n+1}^9	S_{n+1}^{10}	S_{n+1}^{11}	S_{n+1}^{12}
S_n^9	0.369	0.047	−0.029	−0.008	0.007	0.006	0.014	−0.008
S_n^{10}	0.047	0.369	0.029	0.008		0.007	0.046	0.008
S_n^{11}	−0.029	0.029	0.327	−0.027	−0.046	−0.014	−0.024	−0.027
S_n^{12}	−0.008	0.008	−0.027	0.096	−0.012	−0.004	0.006	−0.009

	S_{n+2}^9	S_{n+2}^{10}	S_{n+2}^{11}	S_{n+2}^{12}	S_{n+3}^9	S_{n+3}^{10}	S_{n+3}^{11}	S_{n+3}^{12}
S_n^9				0.004				
S_n^{10}	0.004			0.012				
S_n^{11}			0.003	0.006			−0.002	−0.002
S_n^{12}			−0.002	−0.003				

a) The force constants are directly transferred from those of all-*cis*-transoid tetradecaheptaene calculated at the B3LYP/6-31G* level and uniformly scaled by 0.9128. b) In units of mdyn Å^{-1} for stretching (diagonal) and stretch–stretch interaction (off-diagonal) force constants, mdyn for stretch–bend interaction force constants, and mdyn Å for the other force constants. c) As for the definition of group coordinates, see Table 2. d) Diagonal force constants are underlined. e) Blanks indicate 0.000.

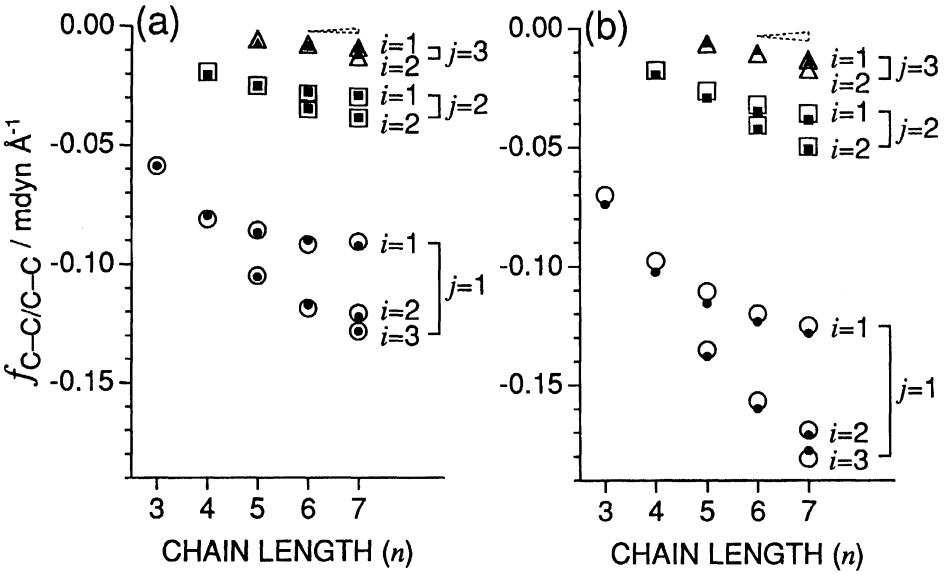

Fig. 9. The scaled C–C stretch/C–C stretch interaction constants ($f_{C-C/C-C}$'s) of (a) all-*cis*-transoid and (b) all-*trans*-cisoid oligoenes as a function of chain length, plotted in a similar way as in Fig. 8. As for the numbering of the $f_{C-C/C-C}$'s, see Fig. 1b.

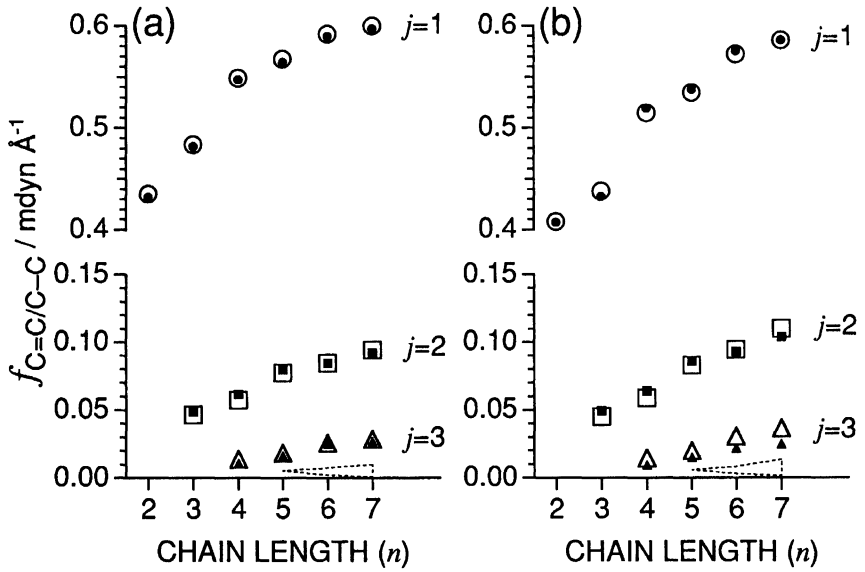

Fig. 10. The scaled C=C stretch/C–C stretch interaction constants ($f_{C=C/C-C}$'s) associated with the central part of (a) all-*cis*-transoid and (b) all-*trans*-cisoid oligoenes as a function of chain length, plotted in a similar way as in Fig. 8. As for the numbering of the $f_{C=C/C-C}$'s, see Fig. 1c.

and ν_3), which are intense in the resonance Raman spectrum, and the CH out-of-plane wagging vibration (ν_{20}), which is strong in the infrared spectrum. However, the wavenumbers for the skeletal stretching vibrations depend not only on the stereostructure, but also on the conjugation length. Therefore, the CH out-of-plane wagging vibration (ν_{20}) seems to be most appropriate for discussing the stereostructure. The wavenumbers for the skeletal stretching vibrations (ν_2 and ν_3) of *Ct* PA are discussed separately in the next subsection.

The observed wavenumbers for ν_{20} are 740 cm^{-1} in a *cis*-$(CH)_x$ film and 548 cm^{-1} in a *cis*-$(CD)_x$ film.[19,26] For *Ct* PA and *Tc* PA, the wavenumbers calculated with force field I are the same as those calculated with force field II. The calculated wavenumbers for ν_{20} are 738 cm^{-1} for *Ct* $(CH)_x$ and 542 cm^{-1} for *Ct* $(CD)_x$. They are in good agreement with the observed values. For *Tc* $(CH)_x$ and *Tc* $(CD)_x$, the calculated wavenumbers (932 and 684 cm^{-1}, respectively) are substantially higher than the observed values. The agreement between the calculated and observed wavenumbers for the other modes are also better for *Ct* PA than for *Tc* PA. Therefore, it is concluded that *cis*-PA films consist of planar *Ct* chains. This conclusion has been drawn by Shirakawa et al.[12] by empirical assignments of the resonance Raman bands. We have confirmed their assignments on the basis of normal coordinate analyses of *Ct* PA and *Tc* PA.

In ν_{20} of *Ct* PA, all of the hydrogen atoms move in the same direction, as shown in Fig. 11. The vibrational pattern of ν_{20} of *Tc* PA is essentially the same. The wavenumber calculated

Table 7. Wavenumbers for the Vibrational Modes of Planar All-*cis*-transoid Polyacetylene and Its Deuterated Analog

Species	Mode[a]		Obsd[b,c] / cm^{-1}		Calcd (scaled)[d] / cm^{-1}		Assignment[e]		
					Force field I	Force field II			
Ct $(CH)_x$	a_g	ν_1	3090		3051	3051	CH str. (100)		
		ν_2	1540	(s)	1489	1542	C=C str. (60)	CH bend (50)	C–C str. (18)
		ν_3	1250	(s)	1215	1250	CH bend (38)	C=C str. (28)	C–C str. (24)
		ν_4	910	(s)	895	892	C–C str. (66)	CCC def. (19)	
	b_{2g}	ν_5	3030		3014	3014	CH str. (101)		
		ν_6			1489	1474	CH bend (70)	C–C str. (32)	
		ν_7	1170		1181	1169	CCC def. (54)	C–C str. (44)	CH bend (31)
		ν_8	755		793	786	CCC def. (79)	C–C str. (37)	
	b_{1u}	ν_9	3044	(‖)	3026	3026	CH str. (101)		
		ν_{10}	1328	(s,‖)	1309	1309	CH bend (106)		
		ν_{11}	448	(s,‖)	434	434	CCC def. (141)	CH bend (11)	
	b_{3u}	ν_{12}	3057	(⊥)	3058	3058	CH str. (99)		
		ν_{13}	1483	(⊥)	1459	1483	C=C str. (95)	CH bend (12)	
		ν_{14}	1246	(⊥)	1228	1228	CH bend (84)		
	b_{1g}	ν_{15}	826		805	805	CH wag. (87)		
	b_{3g}	ν_{16}			925	925	CH wag. (87)	C=C tor. (10)	
		ν_{17}	445		503	503	C=C tor. (102)	CH wag. (34)	
	a_u	ν_{18}	(983)[f]		986	986	CH wag. (57)	C=C tor. (27)	
		ν_{19}	(295)[f]		264	264	C–C tor. (39)	CH wag. (33)	C=C tor. (14)
	b_{2u}	ν_{20}	740	(s,⊥)	738	738	CH wag. (75)	C–C tor. (14)	
Ct $(CD)_x$	a_g	ν_1	2315		2255	2256	CH str. (98)		
		ν_2	1470	(s)	1398	1478	C=C str. (81)	C–C str. (32)	CH bend (21)
		ν_3	976	(s)	965	970	C–C str. (42)	CH bend (39)	
		ν_4	835		813	812	C–C str. (34)	CH bend (32)	CCC def. (15)
	b_{2g}	ν_5	2260		2226	2225	CH str. (98)		
		ν_6			1370	1343	C–C str. (59)	CH bend (32)	
		ν_7	1040		988	987	CCC def. (80)	CH bend (64)	
		ν_8			698	693	CCC def. (45)	C–C str. (34)	CH bend (28)
	b_{1u}	ν_9	2275		2223	2223	CH str. (101)		
		ν_{10}	1050	(s)	1027	1027	CH bend (98)		
		ν_{11}	402	(s)	391	391	CCC def. (134)	CH bend (19)	
	b_{3u}	ν_{12}	2255		2257	2258	CH str. (97)		
		ν_{13}			1439	1462	C=C str. (96)		
		ν_{14}	892		876	876	CH bend (87)		
	b_{1g}	ν_{15}	685		669	669	CH wag. (87)		
	b_{3g}	ν_{16}			791	791	CH wag. (107)		
		ν_{17}	403		417	417	C=C tor. (108)		
	a_u	ν_{18}	(765)[f]		770	770	CH wag. (65)	C=C tor. (23)	
		ν_{19}	(270)[f]		240	240	C–C tor. (41)	CH wag. (25)	C=C tor. (18)
	b_{2u}	ν_{20}	548	(s)	542	542	CH wag. (75)	C–C tor. (14)	

a) The normal modes are classified under the factor group isomorphous to the point group D_{2h}. b) Refs. 6, 9, 19, and 26. c) Terms in parentheses denote intensity (s, strong) and dichroism (‖, parallel band; ⊥, perpendicular band). d) All the force constants are uniformly scaled by 0.9128. e) The numbers represents the values of potential energy distribution (PEDs) calculated with force field II. The sums of PEDs for the two CH stretches, CH bends, CCC deformations, and CH wags in a repeating unit are shown. f) The a_u vibrations are infrared- or Raman-inactive for a regular infinite chain.

for ν_{20} of *Tc* PA is strikingly higher than that of *Ct* PA in spite of their similar vibrational patterns. The difference between the CH wagging force constant of *Ct* PA (0.369 mdyn Å) and that of *Tc* PA (0.384 mdyn Å) is not large enough to account for the large difference between the calculated ν_{20} wavenumber of *Tc* PA and that of *Ct* PA. The PEDs of ν_{20} of *Ct* PA indicate a contribution of the C–C torsion in addition to that of the CH wag (Table 7). Based on symmetry, there is no contribution of the C=C torsion in ν_{20} of *Ct* PA. In ν_{20} of *Tc* PA, on the other hand, the C=C torsion is mixed with the CH wag, but the C–C torsion is not. Therefore, the difference between the wavenumber for ν_{20} of *Ct* PA and that of *Tc* PA is reasonably attributed to the different contributions of the skeletal torsions.

Bates and Baker[23] have observed the infrared spectrum of the single crystal of a *cis*-PA–polystyrene diblock copolymer. In the observed spectrum, intense bands due to the PA blocks have been observed at about 750 and 1000 cm^{-1}. They are in good agreement with the wavenumbers for the CH wags of *Ct* PA and *Tt* PA (740 and 1015 cm^{-1}, respectively[19]). Our calculations on the vibrational spectra of the *Cc* oligoenes indicate that intense bands should appear at about 900 cm^{-1}

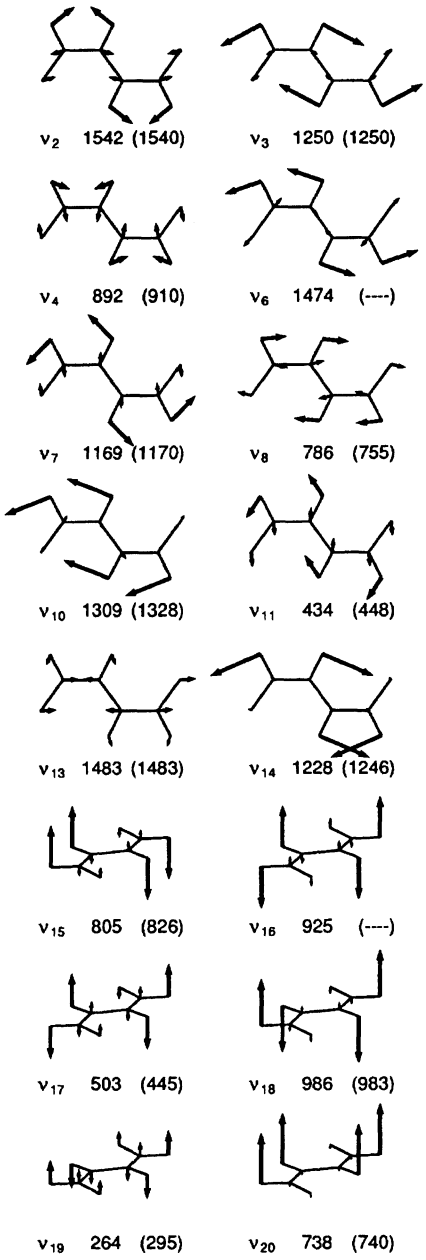

Fig. 11. The vibrational patterns of the infrared- and Raman-active modes of all-*cis*-transoid $(CH)_x$ calculated with force field II. The numbers indicate the calculated and the observed wavenumbers (in parentheses) in cm^{-1}. The observed wavenumbers are taken from Refs. 9, 19, and 26.

Table 8. Wavenumbers Calculated for the Vibrational Modes of Planar All-*trans*-cisoid Polyacetylene and Its Deuterated Analog

Species	Mode[a]		Calcd (scaled)[b] / cm^{-1}	
			Force field I	Force field II
Tc$(CH)_x$	a_g	ν_1	3029	3030
		ν_2	1393	1456
		ν_3	1163	1293
		ν_4	879	880
	b_{2g}	ν_5	3002	3003
		ν_6	1583	1614
		ν_7	1234	1243
		ν_8	809	813
	b_{1u}	ν_9	3014	3014
		ν_{10}	1314	1314
		ν_{11}	430	430
	b_{3u}	ν_{12}	3034	3033
		ν_{13}	1301	1265
		ν_{14}	1174	1161
	b_{1g}	ν_{15}	744	744
	b_{3g}	ν_{16}	897	897
		ν_{17}	266	266
	a_u	ν_{18}	974	974
		ν_{19}	398	398
	b_{2u}	ν_{20}	932	932
Tc$(CD)_x$	a_g	ν_1	2238	2240
		ν_2	1233	1404
		ν_3	1032	1052
		ν_4	757	759
	b_{2g}	ν_5	2221	2224
		ν_6	1500	1537
		ν_7	995	995
		ν_8	716	720
	b_{1u}	ν_9	2214	2214
		ν_{10}	1024	1024
		ν_{11}	390	390
	b_{3u}	ν_{12}	2235	2233
		ν_{13}	1271	1224
		ν_{14}	847	847
	b_{1g}	ν_{15}	621	621
	b_{3g}	ν_{16}	795	795
		ν_{17}	212	212
	a_u	ν_{18}	737	737
		ν_{19}	372	372
	b_{2u}	ν_{20}	684	684

a) The normal modes are classified under the factor group isomorphous to the point group D_{2h}. b) All the force constants are uniformly scaled by 0.9128.

in their infrared spectra. The calculated wavenumbers are 893 cm^{-1} for *Cc* hexatriene, 902 cm^{-1} for *Cc* octatetraene, and 896 cm^{-1} for *Cc* decapentaene. Since the wavenumbers of these bands are almost independent of the chain length, an intense band at about 900 cm^{-1} is expected to appear in the infrared spectra of *Cc* PA. In the observed spectrum of the single crystal, however, no intense band has been observed in the 950—800 cm^{-1} region. From this point also, the existence of the helical *Cc* PA proposed by Bates and Baker[23] is questioned.

Frequencies of the Totally Symmetric Skeletal Vibrations and Conjugation Lengths in All-*cis*-transoid Polyacetylene. The wavenumbers for ν_2 and ν_3 of *Ct* PA calculated with force field I are 1489 and 1215 cm^{-1}, respectively. They are substantially lower than the observed wavenumbers (1540 and 1250 cm^{-1}). When force field II is used, the calculated wavenumbers (1542 and 1250 cm^{-1}) coincide with those observed within 2 cm^{-1}. This coincidence appears to be somewhat puzzling because the skeletal stretching force constants associated with the central parts of the *Ct* oligoenes do not converge at tetradecaheptaene;

i.e., further substantial changes in the values of these force constants are expected on going from tetradecaheptaene to polyacetylene (Figs. 6, 7, 8, 9, and 10). The above result seems to imply that the Raman bands of *cis*-PA originate from *Ct* segments with intermediate conjugation lengths (n being around 7) rather than long *Ct* segments.

The above trend also manifests itself in the chain-length dependence of the vibrational frequencies of the *Ct* oligoenes. For example, the wavenumbers calculated for the C=C stretching modes, which correspond to ν_2 of *Ct* PA, are 1634, 1587, 1574, and 1563 cm^{-1}, respectively, for hexatriene, decapentaene, dodecahexaene, and tetradecaheptaene. For octatetraene, two calculated modes at 1617 and 1597 cm^{-1} seem to have the corresponding character. When these wavenumbers are plotted against $1/(n+1)$, where n is the number of C=C bonds in the oligoenes, they fall on a straight line, parallel to the case of the *Tt* oligoenes.[2] By using this relation, the wavenumber of ν_2 of *Ct* PA has been estimated to be about 1490 cm^{-1}, which is in agreement with the result of a calculation using force field I, but considerably lower than the observed value (1540 cm^{-1}).

One might suspect that these results simply mean that the B3LYP/6-31G* level is inappropriate for the purpose of the present study. However, we have obtained essentially the same result by second-order Møller–Plesset perturbation (MP2) calculations with the 3-21G basis set. We have also extrapolated the structural parameters and force constants of *Tt* PA from those of the *Tt* oligoenes calculated at the B3LYP/6-31G* level. All of the force constants of the *Tt* oligoenes and *Tt* PA were scaled with a single scale factor (0.9128). The wavenumbers of the infrared and Raman bands of *Tt* PA calculated with this structure and force field are in agreement with the observed values to an extent similar to those calculated at the MP2/3-21G and MP2/6-31G* levels.[14] The scale factor determined for *Ct* hexatriene is transferable to *Tt* hexatriene, *Tc* hexatriene, *Tt* octatetraene, *Ct* octatetraene, *Tt* decapentaene, and *Tt* PA. The mean absolute deviations between the calculated and observed wavenumbers (excluding the CH stretching modes) are 12, 11, 11, and 12 cm^{-1} for *Tt* hexatriene, *Tt* octatetraene, *Tt* decapentaene, and *Tt* PA, respectively. (For *Tc* hexatriene and *Ct* octatetraene, see the previous section.) Such agreement between the observed and calculated wavenumbers justifies the use of the same scale factor for *Ct* PA, which in turn ensures the reliability of the scaled force field.

In the following we examine the experimental results in connection with the implication that the observed resonance Raman bands of *cis*-PA appear to originate from *Ct* segments with intermediate conjugation lengths. In the resonance Raman spectra of *trans*-PA, the wavenumbers of the intense bands depend markedly on the wavelength of the excitation.[2—8] This observation, which is usually called the "dispersion", has been regarded as evidence for the existence of *Tt* segments with various conjugation lengths in *trans*-PA films.[2,4,6,8,53,54] Since the electronic absorption maximum of the *Tt* segments shifts to lower energies with increasing conjugation length, the resonance Raman bands observed with red-light excitation are considered to arise from long *Tt* segments, and those observed with blue-light excitation from short *Tt* segments. In the resonance Raman spectra of as-polymerized *cis*-PA, in contrast, none of the intense bands show an appreciable dispersion effect.[2,3,5,8,9] In other words, we cannot observe the resonance Raman bands of long and short *Ct* segments separately by changing the excitation wavelength.

The result that no appreciable dispersion is observed for as-polymerized *cis*-PA is most easily explained, if the wavenumbers for the normal modes of the *Ct* oligoenes, which are expected to give rise to strong resonance Raman bands, are independent of the conjugation length. However, we can rule out this possibility, since the present calculations show that the ν_2 wavenumbers of the *Ct* oligoenes greatly depend on the conjugation length. Another possibility that as-polymerized *cis*-PA consists only of segments with intermediate conjugation lengths centering around $n=7$ is also unlikely. Although *cis*-PA is considered to contain a large number of such segments, in view of the content of *trans* defects[19] (5 to 10 %), it is hard to find a valid reason for the existence of a sharp peak around $n=7$ in the distribution of the conjugation lengths.

When a *cis*-PA sample is thermally isomerized or photoisomerized, *Tt* segments with various conjugation lengths are produced, and *Ct* segments which might have been initially long are converted into *Ct* segments with intermediate or short conjugation lengths.[55] Nevertheless, the resonance Raman bands of *cis*-PA remain almost unchanged in position as chains in *cis*-PA are isomerized from *cis* to *trans*.[4,9,12,29] This result suggests that some mechanism might be at work to enhance the intensities of the Raman bands arising from *Ct* segments with intermediate conjugation lengths.

In connection with the absence of a dispersion effect in the Raman spectra of *cis*-PA, it is worth mentioning the localized excited states of *cis*-PA proposed by Piseri et al.[56] and Tubino et al.[11] These authors have considered that the localized excited states must be responsible for the strong overtones and combinations as well as the broad luminescence bands observed in the resonance Raman spectra of *cis*-PA. The fact that these features cannot be seen in the resonance Raman spectra of *trans*-PA has been interpreted as an indication that the excited states of *Tt* segments associated with the resonance Raman process are delocalized over all segments.

We consider that the above-mentioned localized excited states can also be responsible for the absence of the dispersion effect in *cis*-PA in the following way. The resonance Raman intensity of a totally symmetric vibration of an oligoene or a polyene is primarily determined by structural changes between the ground and excited electronic states associated with the resonance Raman process. The magnitude of the structural change in *cis*-PA upon going from the ground state to the excited state has been quantitatively estimated by Siebrand and Zgierski in an analysis of the resonance Raman excitation profiles.[57] They found that the changes in the carbon–carbon equilibrium distances between the ground and excited states of *cis*-PA are comparable to those of all-*trans*-

β-carotene ($n\approx9$). This leads us to assume that the structural changes in a *Ct* segment are confined to a certain conjugation length (for example, $n\approx7$). If this assumption is true, the electronic absorptions of the *Ct* segments with $n\approx7$ and longer *Ct* segments would arise at about the same wavelength. Furthermore, the electronic absorption band would be dominated by the *Ct* segments with $n\approx7$, because the amount of such segments is expected to be large, as already mentioned. This would mean that the *Ct* segments with $n\approx7$ and longer segments have approximately the same conditions for resonance enhancement of the intensities of their Raman bands. In other words, in resonance with the electronic absorption band of *cis*-PA, not only the intensities of the Raman bands arising from the *Ct* segments with $n\approx7$ are expected to be enhanced, but also those of the Raman bands due to longer *Ct* segments would be enhanced to the extent described above; i.e., the intensities of the Raman bands of the *Ct* segments with $n\approx7$ would never be exceeded by those of the corresponding Raman bands of longer *Ct* segments under any conditions. In analogy with the above consideration for the electronic absorption of *cis*-PA, the Raman spectrum of *cis*-PA would be dominated by contributions from the *Ct* segments with $n\approx7$. Such a situation seems to be in sharp contrast with the case of *trans*-PA consisting of *Tt* segments with various conjugation lengths, whose Raman bands are selectively observed in their respective resonant conditions, which depend on their conjugation length.

Phonon Dispersion Curves of All-*cis*-transoid Polyacetylene. From the discussion given in the previous subsection, it is clear that some ambiguity remains as to the physical meaning of force field II as a force field of an infinite chain. However, from a practical point of view, force field II is useful in that the wavenumbers for the infrared and Raman bands of *cis*-PA can be quantitatively reproduced with this force field. It is therefore expected that force field II would also be useful for analyzing other vibrational spectra of *cis*-PA, i.e., the vibrational spectra of *cis*-copoly ($C_2H_2+C_2D_2$) (in this subsection) and the inelastic neutron scattering spectra of *cis*-PA (in the next subsection).

The phonon dispersion curves and the density of the vibrational states ($g(\nu)$), calculated for *Ct* $(CH)_x$ and *Ct* $(CD)_x$ with force field II, are shown in Figs. 12 and 13. The dispersion curves due to the CH stretches, which are very flat, are not shown. The dispersion curves calculated with force field I are also shown when they are significantly different from those calculated with force field II. Such curves are the ν_2 and ν_3 branches of *Ct* $(CH)_x$ and the ν_2 and ν_{10} branches of *Ct* $(CD)_x$.

In the in-plane acoustic branch, the null-frequency mode at $\delta=0$ corresponds to the translational motion parallel to the chain axis, and that at $\delta=\pi$ to the translational motion perpendicular to the chain axis. In the out-of-plane acoustic branch, the null-frequency mode at $\delta=0$ corresponds to the rotational motion, and that at $\delta=\pi$ to the translational motion.

Shirakawa and Ikeda[19] have observed the infrared spectra of *cis*-copoly ($C_2H_2+C_2D_2$) with various monomer ratios.

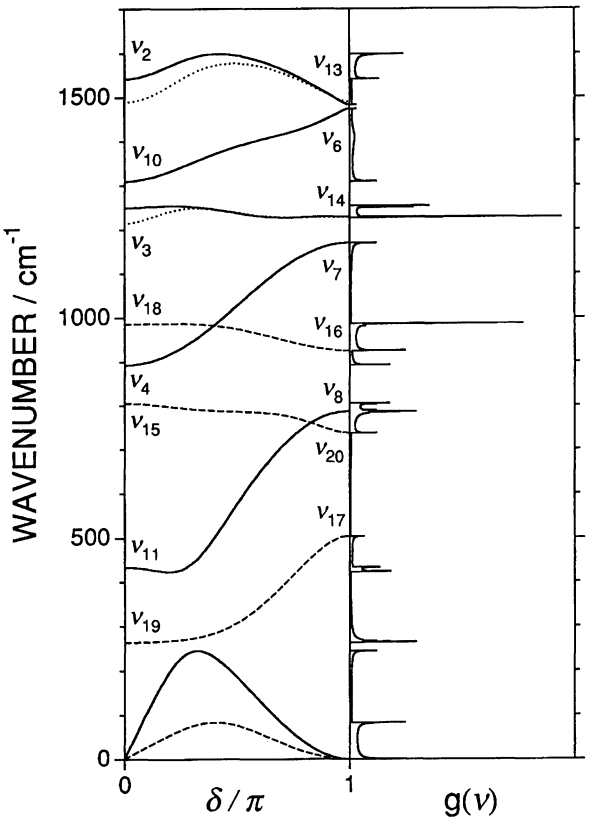

Fig. 12. The phonon dispersion curves and the density of vibrational states (below 1700 cm^{-1}) for the in-plane (solid curves) and out-of-plane (broken curves) vibrations of all-*cis*-transoid $(CH)_x$ calculated with force field II. For ν_2 and ν_3 branches, the dispersion curves calculated with force field I (dotted curves) are also shown.

In the observed spectra, the ν_{20} (CH wag) vibrations exhibit two-mode behavior,[58] indicating that the interaction between the ν_{20} vibrations of the *Ct* $(CH)_x$ and *Ct* $(CD)_x$ segments is negligible. In other words, the density of the vibrational states due to the ν_{20} vibrations of *Ct* $(CH)_x$ and those of *Ct* $(CD)_x$ do not overlap. The $g(\nu)$ profiles calculated in the present study (Figs. 12 and 13) are consistent with this experimental result. Shirakawa and Ikeda[19] have also found that the ν_{20} band of *Ct* $(CH)_x$ observed at 740 cm^{-1} shifts toward higher wavenumbers by about 60 cm^{-1} as the C_2D_2 monomer ratio increases. The ν_{20} band of *Ct* $(CD)_x$ at 548 cm^{-1} also shifts upward to about 650 cm^{-1} as the C_2H_2 monomer ratio increases. These observed spectral changes are consistent with the phonon dispersion curves calculated in the present study. The calculated wavenumber for the ν_{20} branch of *Ct* $(CH)_x$ goes up to about 800 cm^{-1} as the phase difference (δ) decreases from π (Fig. 12). The bands observed at about 800 cm^{-1} in the infrared spectra of the copolymers are assignable to the *Ct* $(CH)_x$ segments, whose conjugation lengths are as short as that of octatetraene. The calculated wavenumber for the ν_{20} branch of *Ct* $(CD)_x$ also increases to about 650 cm^{-1} as δ decreases from π (Fig. 13), which is consistent with the experimental result mentioned above.

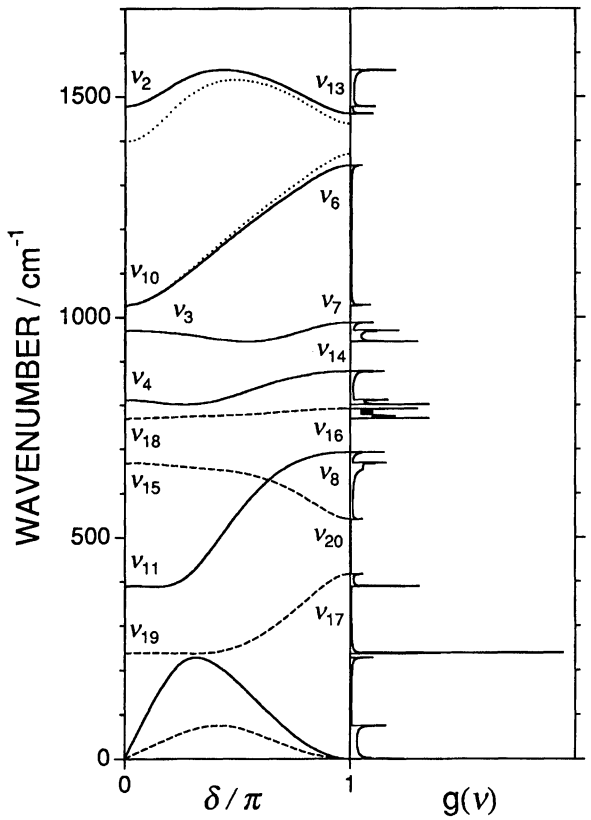

Fig. 13. The phonon dispersion curves and the density of vibrational states (below 1700 cm^{-1}) for the in-plane (solid curves) and out-of-plane (broken curves) vibrations of all-*cis*-transoid $(CD)_x$ calculated with force field II. For ν_2 and ν_{10} branches, the dispersion curves calculated with force field I (dotted curves) are also shown.

Hydrogen-Amplitude-Weighted Density of States of All-*cis*-transoid and All-*trans*-cisoid Polyacetylene. The band intensities in the inelastic neutron scattering (INS) spectra are approximately proportional to the hydrogen-amplitude-weighted density of states ($g_H(\nu)$).[59] The $g_H(\nu)$ profiles of *Ct* $(CH)_x$ and *Tc* $(CH)_x$, calculated with force field II of each isomer, are shown in Fig. 14. Band broadening was taken into account phenomenologically, as in Ref. 14. The observed INS spectrum[33] of *cis*-PA in the 2000—400 cm^{-1} region is shown for comparison in Fig. 14. In the region below 400 cm^{-1}, two INS peaks at 290 and 120 cm^{-1} were observed by a group including one of the present authors,[32] and five peaks at 312, 250, 116, 40, and 12 cm^{-1} were observed by Sauvajol et al.[34] The polarization of some INS peaks have also been observed by Sauvajol et al.[34] with stretch-oriented *cis*-PA films.

The overall profile of the $g_H(\nu)$ of *Ct* $(CH)_x$ is in agreement with the observed INS spectrum, although the calculated peak positions tend to be lower than the observed values. By contrast, the $g_H(\nu)$ profile of *Tc* $(CH)_x$ differs considerably from the observed profile, particularly in the 1450—1250 and 850—700 cm^{-1} regions. Therefore, it is again concluded that *cis*-PA consists of *Ct* chains. The deviations between the peak positions of the calculated $g_H(\nu)$ profile of *Ct* $(CH)_x$ and

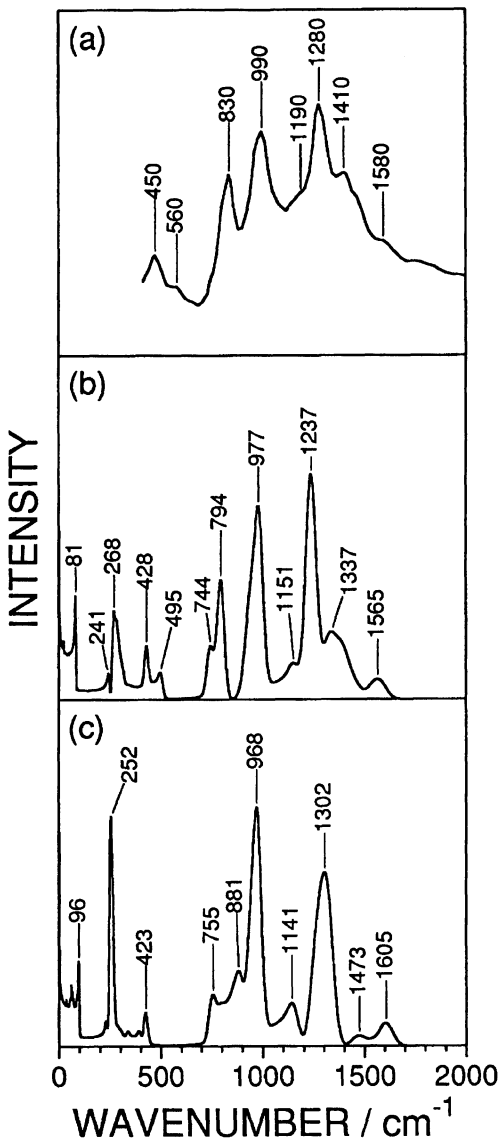

Fig. 14. (a) Observed inelastic neutron scattering spectrum of a *cis*-polyacetylene film (Ref. 33), and the hydrogen-amplitude-weighted density of states of (b) all-*cis*-transoid $(CH)_x$ and (c) all-*trans*-cisoid $(CH)_x$ calculated with force field II of each isomer.

those in the observed spectrum should not be taken seriously, because the error inherent in the observed positions in Ref. 33 is considered to be on the order of 20—30 cm^{-1}.[60]

The weak band at around 1580 cm^{-1} in the observed spectrum is assigned to the ν_2 branch of *Ct* $(CH)_x$. The peak at 1565 cm^{-1} in the calculated $g_H(\nu)$ profile is due to the $\delta=0$ and $\delta\approx\pi/2$ regions of the ν_2 branch. The observed band at 1410 cm^{-1} is assigned to the ν_{10} branch. The calculated peak position is 1337 cm^{-1}. The corresponding peak has been found at 1370 cm^{-1} (170 meV) in the INS spectrum observed by Sauvajol et al.[34] They also found that this band is stronger in the polarization parallel to the chain axis than in the perpendicular polarization. In ν_{10}, all of the hydrogen atoms move in the same direction along the chain axis, as shown in Fig. 11. This vibrational pattern of ν_{10} is consistent

with the polarization of this band. The most intense band observed at 1280 cm^{-1} arises from ν_3 and ν_{14}, where the contribution of the CH in-plane bend is large. In the observed spectrum, a shoulder band is found at 1190 cm^{-1}. Such a feature is also reproduced consistently in the $g_H(\nu)$ profile.

The observed bands in the 1000—700 cm^{-1} region are due to the out-of-plane vibrations. The observed band at 990 cm^{-1} is assigned to the ν_{18} branch, which gives rise to a peak at 977 cm^{-1} in the $g_H(\nu)$ profile. Sauvajol et al.[34] have observed the corresponding band at 970 cm^{-1} (120 meV). This band is strong in the perpendicular polarization. The calculated vibrational patterns of ν_{18} are consistent with the observed polarization of this band. The peak observed at 830 cm^{-1} is ascribed to the ν_{15} branch, in which the contribution of the CH out-of-plane wag is large. The calculated peak position is 794 cm^{-1}.

The weak band observed at 560 cm^{-1} is tentatively assigned to the ν_{17} branch, although the calculated peak position (495 cm^{-1}) seems to be too low. The observed peak at 450 cm^{-1} (427 cm^{-1} according to Ref. 32) is undoubtedly assigned to the ν_{11} branch.

In the $g_H(\nu)$ profile, three peaks at 268, 241, and 81 cm^{-1} can be seen in the region below 300 cm^{-1}. The band at 290 cm^{-1} (reported in Ref. 32) is assignable to the calculated peak at 268 cm^{-1}, which is due to the ν_{19} branch. Sauvajol et al.[34] have observed two bands at 312 and 250 cm^{-1} in the vicinity. Since the 312-cm^{-1} band is strong in the perpendicular polarization, it is due to the ν_{19} branch. Sauvajol et al.[34] have tentatively assigned the 250-cm^{-1} band to the maximum of the in-plane acoustic mode on the basis of its polarization. This assignment seems to be reasonable in view of the present calculations; the corresponding peak is found at 241 cm^{-1} in the $g_H(\nu)$ profile. The observed bands in the region below 150 cm^{-1} are ascribed to the interchain lattice vibrations.[61,62] The calculated peak at 81 cm^{-1}, which is due to the maximum of the out-of-plane acoustic branch, has no corresponding peak in the observed spectrum.

Summary and Conclusion

The total energies of the *Tt*, *Ct*, *Tc*, and *Cc* oligoenes with various chain lengths have been calculated at the B3LYP/6-31G* level. The total energies of the *Tt*, *Ct*, *Tc*, and *Cc* oligoenes with the same chain length increase in this order. The *Cc* oligoenes, which have helical structures, are energetically unfavorable.

Normal coordinate analyses have been performed for *Ct* PA and *Tc* PA. The structures and force fields of *Ct* PA and *Tc* PA have been obtained by analyzing the chain-length dependence and the position dependence of the structural parameters and the force constants of the oligoenes quantitatively. Comparing the wavenumbers calculated for the infrared-active modes and the calculated inelastic neutron scattering spectra with the observed data, we have concluded that *cis*-PA consists of planar *Ct* chains. Although such a conclusion has already been drawn by empirical assignments of the resonance Raman bands of *cis*-PA,[12] we have unambiguously clarified this point on the basis of normal coordinate analyses of *Ct* PA and *Tc* PA. The force fields of *Ct* PA obtained in the present study are useful in quantitatively examining the observed infrared, Raman, and INS spectra. In particular,

Table 9. Parameters in the Functions Approximating the Bond Lengths and Scaled Force Constants of All-*cis*-transoid Oligoenes

	Functional form[a]	Parameter
C=C bond length	(A1)	$a_1=1.374$, $a_2=-0.004365$, $a_3=0.1814$, $a_4=-1.264$, $a_5=-0.02173$, $a_6=-0.2549$
C–C bond length	(A2)	$b_1=1.429$, $b_2=0.007560$, $b_3=0.2171$, $b_4=-1.397$, $b_5=0.02576$, $b_6=0.3243$
C=C stretch	(A3)	$c_1=7.310$, $c_2=0.2590$, $c_3=0.2126$, $c_4=-1.190$, $c_5=0.9500$, $c_6=-0.1835$
C–C stretch	(A4)	$d_1=5.351$, $d_2=-0.1441$, $d_3=0.8495$, $d_4=-1.402$, $d_5=-0.7033$, $d_6=1.297$
C=C stretch / C=C stretch	(A7)	$x_1=-1.072$, $x_2=0.4172$, $x_3=0.6859$, $x_4=-1.003$, $x_5=0.5339$, $x_6=0.5080$, $x_7=-1.232$
C–C stretch / C–C stretch	(A8)	$y_1=-0.5627$, $y_2=0.1198$, $y_3=-0.4548$, $y_4=-1.551$, $y_5=0.5027$, $y_6=0.8355$, $y_7=-1.055$
C=C stretch / C–C stretch	(A9)	$z_1=1.094$, $z_2=-6.124$, $z_3=2.049$, $z_4=-0.02152$, $z_5=0.4210$, $z_6=5.463$, $z_7=-2.110$, $z_8=-0.06239$, $z_9=0.4176$, $z_{10}=-0.9857$, $z_{11}=3.750$, $z_{12}=-1.132$, $z_{13}=25.22$, $z_{14}=-4.451$

a) Numbers correspond to the functional forms given in the Appendix of Ref. 14.

Table 10. Parameters in the Functions Approximating the Bond Lengths, C–C Torsional Angles, and Scaled Force Constants of All-*trans*-cisoid Oligoenes

	Functional form[a]	Parameter
C–C torsional angle	(A1)	$a_1=2.821$, $a_2=16.20$, $a_3=0.6069$, $a_4=-1.138$, $a_5=48.84$, $a_6=1.983$
C=C bond length	(A1)	$a_1=1.377$, $a_2=-0.01031$, $a_3=1.092$, $a_4=-1.446$, $a_5=-0.04172$, $a_6=0.3325$
C–C bond length	(A2)	$b_1=1.429$, $b_2=0.01287$, $b_3=0.4261$, $b_4=-1.465$, $b_5=0.04137$, $b_6=0.4877$
C=C stretch	(A3)	$c_1=6.908$, $c_2=0.6095$, $c_3=1.049$, $c_4=-1.356$, $c_5=1.721$, $c_6=0.1585$
C–C stretch	(A4)	$d_1=5.474$, $d_2=-0.2074$, $d_3=0.4372$, $d_4=-1.485$, $d_5=-0.6920$, $d_6=0.4815$
C=C stretch / C=C stretch	(A7)	$x_1=-0.8535$, $x_2=0.6558$, $x_3=1.627$, $x_4=-0.7975$, $x_5=0.4590$, $x_6=0.6891$, $x_7=-0.9902$
C–C stretch / C–C stretch	(A8)	$y_1=-0.9766$, $y_2=0.3681$, $y_3=0.4355$, $y_4=-1.704$, $y_5=1.633$, $y_6=1.904$, $y_7=-1.006$
C=C stretch / C–C stretch	(A9)	$z_1=1.315$, $z_2=-15.89$, $z_3=5.348$, $z_4=-0.1692$, $z_5=1.181$, $z_6=14.46$, $z_7=-5.470$, $z_8=-0.2422$, $z_9=1.193$, $z_{10}=-0.7098$, $z_{11}=5.366$, $z_{12}=-1.073$, $z_{13}=13.92$, $z_{14}=-4.232$

a) Numbers correspond to the functional forms given in the Appendix of Ref. 14.

most of the observed bands in the INS spectrum have been assigned to the peaks of the calculated $g_H(\nu)$ profile. The wavenumbers calculated for the totally symmetric skeletal vibrations of *Ct* PA are in good agreement with the observed wavenumbers of infrared and Raman bands when the force constants of *Ct* PA are directly transferred from those of *Ct* tetradecaheptaene, although the skeletal stretching force constants do not converge at tetradecaheptaene. This result as well as other experimental results suggests that the observed bands arise from *Ct* segments with intermediate conjugation lengths, rather than long segments.

Appendix

In this Appendix we summarize the functions used to approximate the structural parameters and force constants of the *Ct* and *Tc* oligoenes obtained from density functional calculations. The functional forms used in the present study were taken from our previous study.[14] The functional forms and the values of the parameters determined by a least-squares fitting procedure are given in Table 9 for the *Ct* oligoenes and in Table 10 for the *Tc* oligoenes. The functional forms are numbered according to Ref. 14.

References

1) J. C. W. Chien, "Polyacetylene: Chemistry, Physics, and Material Science," Academic, Orlando (1984).

2) I. Harada, M. Tasumi, H. Shirakawa, and S. Ikeda, *Chem. Lett.*, **1978**, 1411.

3) S. Lefrant, L. S. Lichtmann, H. Temkin, D. B. Fitchen, D. C. Miller, G. E. Whitwell, II, and J. M. Burlitch, *Solid State Commun.*, **29**, 191 (1979).

4) I. Harada, Y. Furukawa, M. Tasumi, H. Shirakawa, and S. Ikeda, *J. Chem. Phys.*,**73**, 4746 (1980).

5) L. S. Lichtmann, A. Sarhangi, and D. B. Fitchen, *Solid State Commun.*, **36**, 869 (1980).

6) H. Kuzmany, *Phys. Status Solidi B*, **97**, 521 (1980).

7) F. B. Schügerl and H. Kuzmany, *J. Chem. Phys.*, **74**, 953 (1981).

8) D. B. Fitchen, *Mol. Cryst. Liq. Cryst.*, **83**, 95 (1982).

9) L. S. Lichtmann, E. A. Imhoff, A. Sarhangi, and D. B. Fitchen, *J. Chem. Phys.*, **81**, 168 (1984).

10) L. Lauchlan, S. Etemad, T.-C. Chung, A. J. Heeger, and A. G. MacDiarmid, *Phys. Rev. B*, **24**, 3701 (1981).

11) R. Tubino, L. Piseri, G. Dellepiane, J. L. Birman, and U. Pedretti, *Solid State Commun.*, **49**, 161 (1984).

12) H. Shirakawa, T. Ito, and S. Ikeda, *Polym. J.*, **4**, 460 (1973).

13) C. R. Fincher, Jr., M. Ozaki, M. Tanaka, D. Peebles, L. Lauchlan, A. J. Heeger, and A. G. MacDiarmid, *Phys. Rev. B*, **20**, 1589 (1979).

14) S. Hirata, H. Torii, and M. Tasumi, *J. Chem. Phys.*, **103**, 8964 (1995).

15) The all-*trans*-cisoid and all-*cis*-cisoid oligoenes have helical structures with the conformations about the C–C bonds being *gauche* rather than *s-cis*. Nevertheless, the abbreviations *Tc* and *Cc* are used throughout the present paper, in order to simplify the notation.

16) G. Lieser, G. Wegner, W. Müller, V. Enkelmann, and W. H. Meyer, *Makromol. Chem., Rapid Commun.*, **1**, 627 (1980).

17) K. Shimamura, F. E. Karasz, J. A. Hirsch, and J. C. W. Chien, *Makromol. Chem., Rapid Commun.*, **2**, 473 (1981).

18) C. R. Fincher, Jr., C.-E. Chen, A. J. Heeger, A. G. MacDiarmid, and J. B. Hastings, *Phys. Rev. Lett.*, **48**, 100 (1982).

19) H. Shirakawa and S. Ikeda, *Polym. J.*, **2**, 231 (1971).

20) R. H. Baughman, S. L. Hsu, G. P. Pez, and A. J. Signorelli, *J. Chem. Phys.*, **68**, 5405 (1978).

21) G. Lieser, G. Wegner, W. Müller, and V. Enkelmann, *Makromol. Chem., Rapid Commun.*, **1**, 621 (1980).

22) a) J. C. W. Chien, F. E. Karasz, and K. Shimamura, *J. Polym. Sci. Polym. Lett. Ed.*, **20**, 97 (1982); b) *Macromolecules*, **15**, 1012 (1982).

23) F. S. Bates and G. L. Baker, *Macromolecules*, **16**, 1013 (1983).

24) M. L. Elert and C. T. White, *Phys. Rev. B*, **28**, 7387 (1983).

25) a) B. K. Rao, J. A. Darsey, and N. R. Kestner, *J. Chem. Phys.*, **79**, 1377 (1983); b) *Phys. Rev. B*, **31**, 1187 (1985).

26) a) P. Piaggio, G. Dellepiane, L. Piseri, R. Tubino, and C. Taliani, *Solid State Commun.*, **50**, 947 (1984); b) P. Piaggio, G. Dellepiane, R. Tubino, L. Piseri, G. Zannoni, G. Zerbi, and G. Lugli, *J. Mol. Struct.*, **115**, 193 (1984).

27) E. Faulques, J.-P. Buisson, and S. Lefrant, *Phys. Rev. B*, **52**, 15039 (1995).

28) K. Tanaka, T. Koike, K. Yoshizawa, K. Ohzeki, and T. Yamabe, *Solid State Commun.*, **49**, 165 (1984).

29) M. Tasumi, H. Yoshida, M. Fujiwara, H. Hamaguchi, and H. Shirakawa, *Synth. Met.*, **17**, 319 (1987).

30) E. Perrin, E. Faulques, S. Lefrant, E. Mulazzi, and G. Leising, *Phys. Rev. B*, **38**, 10645 (1988).

31) G. Lanzani, S. Luzzati, R. Tubino, and G. Dellepiane, *J. Chem. Phys.*, **91**, 732 (1989).

32) M. Tasumi, I. Harada, H. Takeuchi, H. Shirakawa, S. Suzuki, A. Maconnachie, and A. J. Dianoux, *Synth. Met.*, **10**, 293 (1985).

33) A. Maconnachie, A. J. Dianoux, H. Shirakawa, and M. Tasumi, *Synth. Met.*, **14**, 323 (1986).

34) a) J. L. Sauvajol, D. Djurado, A. J. Dianoux, N. Theophilou, and J. E. Fischer, *Phys. Rev. B*, **43**, 14305 (1991); b) A. J. Dianoux, G. R. Kneller, J. L. Sauvajol, and J. C. Smith, *J. Chem. Phys.*, **99**, 5586 (1993).

35) M. Galtier, C. Benoit, and A. Montaner, *Mol. Cryst. Liq. Cryst.*, **83**, 1141 (1982).

36) C. Benoit, M. Galtier, and A. Montaner, *J. Phys. Chem. Solids*, **45**, 275 (1984).

37) D. Raković, I. Božović, L. A. Gribov, S. A. Stepanyan, and V. A. Dementiev, *Phys. Rev. B*, **29**, 3412 (1984).

38) H. Teramae, T. Yamabe, and A. Imamura, *J. Chem. Phys.*, **81**, 3564 (1984).

39) a) A. Girlando, A. Painelli, and Z. G. Soos, *J. Chem. Phys.*, **98**, 7459 (1993); b) A. Girlando, A. Painelli, G. W. Hayden, and Z. G. Soos, *Chem. Phys.*, **184**, 139, (1994).

40) P. G. Szalay, A. Karpfen, and H. Lischka, *J. Chem. Phys.*, **87**, 3530 (1987).

41) M. J. Frisch, G. W. Trucks, H. B. Schlegel, P. M. W. Gill, B. G. Johnson, M. A. Robb, J. R. Cheeseman, T. A. Keith, G. A. Petersson, J. A. Montgomery, K. Raghavachari, M. A. Al-Laham, V. G. Zakrzewski, J. V. Ortiz, J. B. Foresman, J. Cioslowski, B. B. Stefanov, A. Nanayakkara, M. Challacombe, C. Y. Peng, P. Y. Ayala, W. Chen, M. W. Wong, J. L. Andres, E. S. Replogle, R. Gomperts, R. L. Martin, D. J. Fox, J. S. Binkley, D. J. Defrees, J. Baker, J. P. Stewart, M. Head-Gordon, C. Gonzalez, and J. A. Pople, "Gaussian 94," Gaussian, Inc., Pittsburgh, Pennsylvania (1995).

42) H. Yoshida, Y. Furukawa, and M. Tasumi, *J. Mol. Struct.*, **194**, 279 (1989).

43) M. Hossain, B. E. Kohler, and P. West, *J. Phys. Chem.*, **86**, 4918 (1982).

44) Y. Furukawa, H. Takeuchi, I. Harada, and M. Tasumi, *J. Mol. Struct.*, **100**, 341 (1983).
45) T. Nakagawa and Y. Oyanagi, "SALS" in "Recent Developments in Statistical Inference and Data Analysis," ed by K. Matsushita, North Holland, Amsterdam (1980), p. 221.
46) S. Karabunarliev, *J. Phys. Chem.*, **99**, 14566 (1995).
47) "IUPAC Commission on Molecular Structure and Spectroscopy," *Pure Appl. Chem.*, **50**, 1707 (1978).
48) P. W. Higgs, *Proc. R. Soc. (London), Ser. A*, **A220**, 472 (1953).
49) Y. Yamakita, "LXVIEW, version 1.00," The University of Tokyo (1994).
50) H. Teramae, *J. Chem. Phys.*, **85**, 990 (1986).
51) C. S. Yannoni and T. C. Clarke, *Phys. Rev. Lett.*, **51**, 1191 (1983).
52) a) S. Suhai, *Chem. Phys. Lett.*, **96**, 619 (1983); b) *Phys. Rev. B*, **27**, 3506 (1983).
53) H. Kuzmany, *J. Phys. (Paris) Colloq.*, **C3**, 255 (1983).
54) a) B. E. Kohler and I. D. W. Samuel, *J. Chem. Phys.*, **103**, 6248 (1995); b) B. E. Kohler and J. C. Woehl, *J. Chem. Phys.*, **103**, 6253 (1995).
55) H. W. Gibson, S. Kaplan, R. A. Mosher, W. M. Prest, Jr., and R. J. Weagley, *J. Am. Chem. Soc.*, **108**, 6843 (1986).
56) L. Piseri, R. Tubino, and E. Mulazzi, *Mol. Cryst. Liq. Cryst.*, **83**, 135 (1982).
57) W. Siebrand and M. Z. Zgierski, *J. Chem. Phys.*, **81**, 185 (1984).
58) H. Takeuchi, Y. Furukawa, I. Harada, and H. Shirakawa, *J. Chem. Phys.*, **80**, 2925 (1984).
59) J. Howard and T. C. Waddington, in "Advances in Infrared and Raman Spectroscopy," ed by R. J. H. Clark and R. E. Hester, Heyden, London (1980), Vol. 7, p. 86.
60) S. Hirata, H. Torii, Y. Furukawa, M. Tasumi, and J. Tomkinson, *Chem, Phys, Lett.*, in press.
61) G. Bechtold, L. Genzel, and S. Roth, *Solid State Commun.*, **53**, 1 (1985).
62) H. Ohta, M. Kojima, K. Nagasaka, and T. Ishii, *Mol. Cryst. Liq. Cryst.*, **158B**, 291 (1988).